

1 **Cross-species complementation reveals conserved functions for EARLY FLOWERING 3**
2 **between monocots and dicots.**

3
4 He Huang¹, Malia Gehan¹, Sarah E. Huss², Sophie Alvarez^{1,4}, Cesar Lizarraga¹, Ellen L.
5 Gruebbling³, John Grier¹, Michael J. Naldrett^{1,4}, Rebecca K. Bindbeutel¹, Bradley S. Evans¹,
6 Todd C. Mockler¹, and Dmitri A. Nusinow^{1*}

7
8 ¹ Donald Danforth Plant Science Center, St. Louis, MO, 63132, USA

9 ² Webster University, Webster Groves, MO, 63119, USA

10 ³ Saint Louis University, St. Louis, MO, 63103, USA

11 ⁴ Present address: University of Nebraska-Lincoln, Lincoln, NE, 68588, USA

12 *To whom correspondence should be addressed meter@danforthcenter.org

13

14
15
16
17
18
19
20
21
22
23
24
25
26
27
28
29
30
31
32
33
34

Abstract

Plant responses to the environment are shaped by external stimuli and internal signaling pathways. In both the model plant *Arabidopsis thaliana* and crop species, circadian clock factors have been identified as critical for growth, flowering and circadian rhythms. Outside of *A. thaliana*, however, little is known about the molecular function of clock genes. Therefore, we sought to compare the function of *Brachypodium distachyon* and *Setaria viridis* orthologs of *EARLY FLOWERING3*, a key clock gene in *A. thaliana*. To identify both cycling genes and putative ELF3 functional orthologs in *S. viridis*, a circadian RNA-seq dataset and online query tool (Diel Explorer) was generated as a community resource to explore expression profiles of *Setaria* genes under constant conditions after photo- or thermo-entrainment. The function of *ELF3* orthologs from *A. thaliana*, *B. distachyon*, and *S. viridis* were tested for complementation of an *elf3* mutation in *A. thaliana*. Despite comparably low sequence identity versus AtELF3 (less than 37%), both monocot orthologs were capable of rescuing hypocotyl elongation, flowering time and arrhythmic clock phenotypes. Molecular analysis using affinity purification and mass spectrometry to compare physical interactions also found that BdELF3 and SvELF3 could be integrated into similar complexes and networks as AtELF3, including forming a composite evening complex. Thus, we find that, despite 180 million years of separation, BdELF3 and SvELF3 can functionally complement loss of *ELF3* at the molecular and physiological level.

35

36 **Introduction**

37

38 Plants have developed sophisticated signaling networks to survive and thrive in diverse
39 environments. Many plant responses are shaped, in part, by an internal timing mechanism known
40 as the circadian clock, which allows for the coordination and anticipation of daily and seasonal
41 variation in the environment (Greenham and McClung, 2015). Circadian clocks, which are
42 endogenous oscillators with a period of approximately 24 hours, are critical for regulating the
43 timing of physiology, development, and metabolism in all domains of life (Bell-Pedersen et al.,
44 2005; Doherty and Kay, 2010; Edgar et al., 2012; Harmer, 2009; Wijnen and Young, 2006). In
45 plants and blue-green algae, circadian clocks provide an experimentally observable adaptive
46 advantage by synchronizing internal physiology with external environmental cues (Dodd et al.,
47 2005; Ouyang et al., 1998; Woelfle et al., 2004). Currently, circadian oscillators are best
48 understood in the reference plant *Arabidopsis thaliana*, in which dozens of clock or clock-
49 associated components have been identified using genetic screens and non-invasive, luciferase-
50 based oscillating reporters (Hsu and Harmer, 2014; Nagel and Kay, 2012). These morning-,
51 afternoon-, and evening-phased clock oscillators form multiple interconnected transcription-
52 translation feedback loops and compose a complex network (Hsu and Harmer, 2014; Pokhilko et
53 al., 2012). The *A. thaliana* circadian clock regulates a significant portion of physiology,
54 including photosynthesis, growth, disease resistance, starch metabolism, and phytohormone
55 pathways (Covington et al., 2008; Graf et al., 2010; Harmer et al., 2000; Michael et al., 2008;
56 Wang et al., 2011b), with up to 30% of gene expression under circadian control (Covington et
57 al., 2008; Michael et al., 2008).

58 Within the *Arabidopsis* clock network, a tripartite protein complex called the evening complex
59 (EC) is an essential component of the evening transcription loop (Huang and Nusinow, 2016b).
60 The EC consists of three distinct proteins, EARLY FLOWERING 3 (ELF3), EARLY
61 FLOWERING 4 (ELF4) and LUX ARRHYTHMO (LUX, also known as PHYTOCLOCK1),
62 with transcript and protein levels peaking in the evening (Doyle et al., 2002; Hazen et al., 2005;
63 Hicks et al., 2001; Nusinow et al., 2011; Onai and Ishiura, 2005). The EC plays a critical role in
64 maintaining circadian rhythms, by repressing expression of key clock genes (Dixon et al., 2011;
65 Helfer et al., 2011; Herrero et al., 2012; Kolmos et al., 2011; Mizuno et al., 2014). Loss-of-
66 function mutation of any EC component in *A. thaliana* results in arrhythmicity of the circadian
67 clock and causes excessive cellular elongation and early flowering regardless of environmental
68 photoperiod (Doyle et al., 2002; Hazen et al., 2005; Hicks et al., 2001; Khanna et al., 2003; Kim
69 et al., 2005; Nozue et al., 2007; Nusinow et al., 2011; Onai and Ishiura, 2005).

70

71 In *A. thaliana*, ELF3 directly interacts with ELF4 and LUX, functioning as a scaffold to bring
72 ELF4 and LUX together (Herrero et al., 2012; Nusinow et al., 2011). Additional protein-protein

73 interaction studies and tandem affinity purification coupled with mass spectrometry (AP-MS)
74 have identified many ELF3-associating proteins and established ELF3 as a hub of a complex
75 protein-protein interaction network, which consists of key components from the circadian clock
76 pathway and light signaling pathways (Huang et al., 2016a; Huang and Nusinow, 2016b; Liu et
77 al., 2001; Yu et al., 2008). In this network, ELF3 directly interacts with the major red light
78 photoreceptor phytochrome B (phyB), and CONSTITUTIVE PHOTOMORPHOGENIC 1
79 (COP1), which is an E3 ubiquitin ligase required for proper regulation of photomorphogenesis
80 and also interacts with phyB (Liu et al., 2001; Yu et al., 2008). The physical interaction among
81 ELF3, phyB, and COP1, together with recruitment of direct interacting proteins to the network,
82 provides biochemical evidence for cross-talk between circadian clock and light signaling
83 pathways (Huang and Nusinow, 2016b). Although much work does translate from *A. thaliana* to
84 other plant species, interaction between ELF3 and other proteins have yet to be tested in species
85 outside *A. thaliana*. Whether evening complex-like protein assemblages or a similar ELF3-
86 containing protein-protein interaction network exists in species outside *A. thaliana* is an
87 interesting question to ask.

88

89 Identification and characterization of clock genes in diverse plant species has revealed that many
90 clock components are broadly conserved (Filichkin et al., 2011; Khan et al., 2010; Lou et al.,
91 2012; Song et al., 2010). Furthermore, comparative genomics analysis has found that circadian
92 clock components are selectively retained after genome duplication events, suggestive of the
93 importance of their role in maintaining fitness (Lou et al., 2012). Recently, mutant alleles of
94 *ELF3* were identified associated with the selection of favorable photoperiodism phenotypes in
95 several crops, such as pea, rice, soybean and barley (Faure et al., 2012; Lu et al., 2017;
96 Matsubara et al., 2012; Saito et al., 2012; Weller et al., 2012; Zakhrabekova et al., 2012). These
97 findings are consistent with the reported functions of *A. thaliana* ELF3 in regulating the
98 photoperiodic control of growth and flowering (Hicks et al., 2001; Huang and Nusinow, 2016b;
99 Nozue et al., 2007; Nusinow et al., 2011). However, opposed to the early flowering phenotype
100 caused by *elf3* mutants in *A. thaliana*, pea, and barley (Faure et al., 2012; Hicks et al., 2001;
101 Weller et al., 2012), loss of function mutation of the rice or soybean *ELF3* ortholog results in
102 delayed flowering (Lu et al., 2017; Saito et al., 2012), suggesting ELF3-mediated regulation of
103 flowering varies in different plant species. The molecular mechanisms underlying this difference
104 have not been thoroughly elucidated.

105

106 *Brachypodium distachyon* is a C3 model grass closely related to wheat, barley, oats, and rice.
107 *Setaria viridis*, is a C4 model grass closely related to maize, sorghum, sugarcane, and other
108 bioenergy grasses. Both grasses are small, transformable, rapid-cycling plants with recently
109 sequenced genomes, making them ideal model monocots for comparative analysis with
110 *Arabidopsis* (Bennetzen et al., 2012; Brutnell et al., 2010). Computational analysis of *B.*
111 *distachyon* has identified putative circadian clock orthologs (Higgins et al., 2010), including

112 *BdELF3*. However, no such comparative analysis has been done systematically in *S. viridis* to
113 identify putative orthologs of circadian clock genes. Therefore, we generated a RNA-seq time-
114 course dataset to analyze the circadian transcriptome of *S. viridis* after either photo- or thermo-
115 entrainment and developed an online gene-expression query tool (Diel Explorer) for the
116 community. We found that the magnitude of circadian regulated genes in *S. viridis* is similar to
117 other monocots after photo-entrainment, but much less after thermal entrainment. We further
118 analyzed the functional conservation of SvELF3, together with previously reported BdELF3, by
119 introducing both ELF3 orthologs into *A. thaliana elf3* mutant for physiological and biochemical
120 characterization. We found that *B. distachyon* and *S. viridis* ELF3 can complement the hypocotyl
121 elongation, flowering time and circadian arrhythmia phenotypes caused by the *elf3* mutation in
122 *A. thaliana*. Furthermore, AP-MS analyses found that *B. distachyon* and *S. viridis* ELF3 were
123 integrated into a similar protein-protein interaction network *in vivo* as their *A. thaliana*
124 counterpart. Our data collectively demonstrated the functional conservation of ELF3 among *A.*
125 *thaliana*, *B. distachyon* and *S. Viridis* is likely due to the association with same protein partners,
126 providing insights of how ELF3 orthologs potentially function in grasses.

127

128 **Materials and methods**

129

130 *Plant Materials and Growth Conditions*

131

132 For *A. thaliana*, wild type (Columbia-0) and *elf3-2* plants carrying the CCA1::LUC reporter were
133 described previously (Nusinow et al., 2011; Pruneda-Paz et al., 2009). Seeds were surface
134 sterilized and plated on 1/2x Murashige and Skoog (MS) basal salt medium with 0.8% agar + 1%
135 (w/v) sucrose. After 3 days of stratification, plates were placed horizontally in a Percival
136 incubator (Percival Scientific, Perry, IA), supplied with 80 $\mu\text{mol m}^{-2} \text{sec}^{-1}$ white light and set to a
137 constant temperature of 22°C. Plants were grown under 12 h light / 12 h dark cycles (12L:12D)
138 for 4 days (for physiological experiments) or for 10 days (for AP-MS) before assays.

139

140 For *S. viridis* circadian expression profiling by RNA-seq, seeds were stratified for 5 days at 4°C
141 before being moved to entrainment conditions. Plants were grown under either LDHH or LLHC
142 (L: light, D: dark, H: hot, C: cold) entrainment condition, and then sampled for RNA-seq in
143 constant light and constant temperature (32°C) conditions (F, for free-running) every 2 hours for
144 48 hours. Light intensity was set to 400 $\mu\text{mol m}^{-2} \text{sec}^{-1}$ white light. In LDHH-F, stratified *S.*
145 *viridis* seeds were grown for 10 days under 12L:12D and constant temperature (32°C) before
146 sampling in constant light and constant temperature. In LLHC-F, stratified *S. viridis* seeds were
147 grown for 10 days under constant light conditions and cycling temperature conditions 12 h at
148 32°C (subjective day) / 12 h at 22°C (subjective night) before sampling in constant conditions.
149 Two experimental replicates were collected for each entrainment condition.

150

151 *Setaria Circadian RNA-seq*

152

153 The second leaf from the top of seventeen *S. viridis* plants was selected for RNA-seq sampling at
154 each time point for each sampling condition. Five replicate samples were pooled after being
155 ground in liquid nitrogen and resuspended in lithium chloride lysis binding buffer (Wang et al.,
156 2011a). RNA-seq libraries from leaf samples were constructed according to the previous
157 literature (Wang et al., 2011a) with one major modification. Rather than extracting RNA then
158 mRNA from ground leaf samples (Wang et al., 2011a), mRNA was extracted directly from
159 frozen ground leaf samples similar to the method described in (Kumar et al., 2012), except that
160 two additional rounds of wash, binding, and elution steps after treatment with EDTA were
161 necessary to remove rRNA from samples. mRNA quantity was assessed using a Qubit with a
162 Qubit RNA HS Kit and mRNA quality was assessed using a Bioanalyzer and Plant RNA PiCO
163 chip. 96 library samples were multiplexed 12 per lane, for a total of 8 lanes of Illumina HiSeq
164 2000 sequencing. Paired end 101 bp Sequencing was done at MOgene (St. Louis, MO). Raw
165 data can be found on the Short Read Archives (SRA) at [PRJNA31286](https://www.ncbi.nlm.nih.gov/sra/PRJNA31286).

166

167 RNA-seq data was trimmed with BBTools (v36.20) using parameters: ktrim=r k=23 mink=11
168 hdist=1 tpe tbo ktrim=l k=23 mink=11 hdist=1 tpe tbo qtrim=rl trimq=20 minlen=20 (Bushnell,
169 2016). Any parameters not specified were run as default. Before trimming we had 1,814,939,650
170 reads with a mean of 18,905,621 reads per sample and a standard deviation of 2,875,187. After
171 trimming, we have 1,646,019,593 reads with a mean of 17,146,037 reads per sample and a
172 standard deviation of 2,411,061. Kallisto (v 0.42.4; (Bray et al., 2016)) was used to index the
173 transcripts with the default parameters and the *S. viridis* transcripts fasta file (Sviridis_311_v1.1)
174 from Phytozome (Goodstein et al., 2012). The reads were quantified with parameters:-t 40 -b
175 100. Any parameters not specified were run as default. Kallisto output was formatted for
176 compatibility with JTKCycle (v3.1; (Hughes et al., 2010)) and circadian cycles were detected.
177 To query the *S. viridis* expression data we developed Diel Explorer. The tool can be found at
178 <http://shiny.bioinformatics.danforthcenter.org/diel-explorer/>. Underlying code for Diel Explorer
179 is available on Github (<https://github.com/maliagehan/diel-explorer>).

180

181 *Plasmid Constructs and Generation of Transgenic Plants*

182

183 Coding sequences (without the stop codon) of *AtELF3* (*AT2G25930*) and *SvELF3a*
184 (*Sevir.5G206400.1*) were cloned into the pENTR/D-TOPO vector (ThermoFisher Scientific,
185 Waltham, MA), verified by sequencing and were recombined into the pB7HFC vector (Huang et
186 al., 2016a) using LR Clonease (ThermoFisher Scientific, Waltham, MA). Coding sequence of
187 *BdELF3* (*Bradi2g14290.1*) was submitted to the U.S. Department of Energy Joint Genome
188 Institute (DOE-JGI), synthesized by the DNA Synthesis Science group, and cloned into the
189 pENTR/D-TOPO vector. Sequence validated clones were then recombined into pB7HFC as

190 described above. The pB7HFC-At/Bd/SvELF3 constructs were then transformed into *elf3-2*
191 [*CCA1::LUC*] plants by the floral dip method (Zhang et al., 2006). Homozygous transgenic
192 plants were validated by testing luciferase bioluminescence, drug resistance, and by PCR-based
193 genotyping. All primers used in this paper were listed in Supplemental Table 1.

194

195 *Hypocotyl and Flowering Time Measurement*

196

197 20 seedlings of each genotype were arrayed and photographed with a ruler for measuring
198 hypocotyl length using the ImageJ software (NIH) (Schneider et al., 2012). The procedure was
199 repeated three times. For measuring flowering time, 12 plants of each genotype were placed in a
200 random order and were grown under the long day condition (light : dark = 16 : 8 hours). The
201 seedlings were then observed every day at 12:00 PM; the date on which each seedling began
202 flowering, indicated by the growth of a ~1 cm inflorescence stem, was recorded along with the
203 number of rosette leaves produced up to that date.

204

205 *Circadian Assays in A. thaliana*

206

207 Seedlings were transferred to fresh 1/2x MS plates after 5 days of entrainment under the
208 12L:12D condition and sprayed with sterile 5 mM luciferin (Gold Biotechnology, St. Louis, MO)
209 prepared in 0.1% (v/v) Triton X-100 solution. Sprayed seedlings were then imaged in constant
210 light ($70 \mu\text{mol m}^{-2} \text{sec}^{-1}$, wavelengths 400, 430, 450, 530, 630, and 660 set at intensity 350
211 (Heliospectra LED lights, Göteborg, Sweden)). Bioluminescence was recorded after a 120-180s
212 delay to diminish delayed fluorescence (Gould et al., 2009) over 5 days using an ultra-cooled
213 CCD camera (Pixis 1024B, Princeton Instruments) driven by Micro-Manager software (Edelstein
214 et al., 2010; Edelstein et al., 2014). The images were processed in stacks by Metamorph software
215 (Molecular Devices, Sunnyvale, CA), and rhythms determined by fast Fourier transformed non-
216 linear least squares (FFT-NLLS) (Plautz et al., 1997) using the interface provided by the
217 Biological Rhythms Analysis Software System 3.0 (BRASS) available at <http://www.amillar.org>.

218

219 *Yeast Two-Hybrid Analysis*

220

221 Yeast two-hybrid assays were carried out as previously described (Huang et al., 2016a). In brief,
222 the DNA binding domain (DBD) or activating domain (AD)-fused constructs were transformed
223 using the Li-Ac transformation protocol (Clontech) into *Saccharomyces cerevisiae* strain Y187
224 (MAT α) and the AH109 (MATa), respectively. Two strains of yeast were then mated to generate
225 diploid with both DBD and AD constructs. Protein-protein interaction was tested in diploid yeast
226 by replica plating on CSM –Leu –Trp –His media supplemented with extra Adenine (30mg/L
227 final concentration) and 2mM 3-Amino-1,2,4-triazole (3AT). Pictures were taken after 4-day

228 incubation at 30 °C. All primers used for cloning plasmid constructs were listed in Supplemental
229 Table 1.

230

231 *Protein Extraction and Western Blotting*

232

233 Protein extracts were made from 10-day-old seedlings as previously described (Huang et al.,
234 2016a) and loaded 50 µg to run 10% SDS-PAGE. For western blots, all of the following primary
235 and secondary antibodies were diluted into PBS + 0.1% Tween and incubated at room
236 temperature for 1 hour: anti-FLAG®M2-HRP (Sigma, A8592, diluted at 1:10,000) and anti-
237 Rpt5-rabbit (ENZO Life Science, BML-PW8245-0025, diluted at 1:5000) and anti-Rabbit-HRP
238 secondary antibodies (Sigma, A0545, diluted at 1:10,000).

239

240 *Affinity Purification and Mass Spectrometry*

241

242 Protein extraction methods and protocols for AP-MS were described previously (Huang et al.,
243 2016a; Huang and Nusinow, 2016a; Huang et al., 2016c). In brief, transgenic seedlings carrying
244 the At/Bd/SvELF3-HFC constructs were grown under 12L:12D conditions for 10 days and were
245 harvested at dusk (ZT12). 5 grams of seedlings were needed per replicate to make protein
246 extracts, which underwent tandem affinity purification utilizing the FLAG and His epitopes of
247 the fusion protein. Purified samples were reduced, alkylated and digested by trypsin. The tryptic
248 peptides were then injected to an LTQ-Orbitrap Velos Pro (ThermoFisher Scientific, Waltham,
249 MA) coupled with a U3000 RSLCnano HPLC (ThermoFisher Scientific, Waltham, MA) with
250 settings described previously (Huang et al., 2016a).

251

252 *AP-MS Data analysis*

253

254 Data analysis was done as previously described (Huang et al., 2016a). The databases searched
255 were TAIR10 database (20101214, 35,386 entries) and the cRAP database
256 (<http://www.thegpm.org/cRAP/>). Peptide identifications were accepted if they could be
257 established at greater than 95.0% probability and the Scaffold Local FDR was <1%. Protein
258 identifications were accepted if they could be established at greater than 99.0% probability as
259 assigned by the Protein Prophet algorithm (Keller et al., 2002; Nesvizhskii et al., 2003). A full
260 list of all identified proteins (reporting total/exclusive unique peptide count and percent
261 coverage) can be found in Supplemental Table 2. The mass spectrometry proteomics data have
262 been deposited to the ProteomeXchange Consortium (Vizcaino et al., 2014) via the PRIDE
263 partner repository with the dataset identifier PXD006352 and 10.6019/PXD006352.

264

265 **Results**

266

267 *Identifying and Cloning ELF3 Orthologs from B. distachyon and S. viridis*

268

269 ELF3 is a plant-specific nuclear protein with conserved roles in flowering and the circadian
270 clock in multiple plant species (Faure et al., 2012; Herrero et al., 2012; Liu et al., 2001; Lu et al.,
271 2017; Matsubara et al., 2012; Saito et al., 2012; Weller et al., 2012; Zakhrabekova et al., 2012).
272 To identify ELF3 orthologs in monocots, we used the protein sequence of *Arabidopsis thaliana*
273 ELF3 (AtELF3) to search the proteomes of two model monocots *Brachypodium distachyon* and
274 *Setaria viridis* using BLAST (Altschul et al., 1990). Among the top hits, we identified a
275 previously reported ELF3 homolog in *B. distachyon* (*Bradi2g14290.1*, *BdELF3*) (Calixto et al.,
276 2015; Higgins et al., 2010) and two putative *ELF3* homologous genes *Sevir.5G206400.1*
277 (referred as *SvELF3a*) and *Sevir.3G123200.1* (referred as *SvELF3b*) in *S. viridis*. We used
278 Clustal Omega (<http://www.ebi.ac.uk/Tools/msa/clustalo/>) to conduct multiple sequence
279 alignments of comparing protein sequences of ELF3 orthologs with that of AtELF3 (Sievers et
280 al., 2011). *BdELF3*, *SvELF3a* and *SvELF3b* encode proteins with similar identity compared to
281 AtELF3 (34.7–36.8%) (Supplemental Figure 1). When compared to *BdELF3*, *SvELF3b* was
282 74.3% identical while *SvELF3a* was 57.4% identical (Supplemental Figure 1). Therefore, to
283 maximize the diversity of ELF3 sequences used in this study, we cloned full length cDNAs
284 encoding *BdELF3* and *SvELF3a*.

285

286 *Diel Explorer of S. viridis Circadian Data.*

287

288 In *Arabidopsis*, ELF3 cycles under diel and circadian conditions (constant condition after
289 entrainment) with a peak phase in the evening (Covington et al., 2001; Hicks et al., 2001;
290 Nusinow et al., 2011). We queried an available diurnal time course expression dataset for *B.*
291 *distachyon* from the DIURNAL website, and found that *BdELF3* expression cycles under diel
292 conditions (LDHH, 12 h light / 12 h dark cycles with constant temperature), but not under
293 circadian conditions in available data (LDHC-F or LDHH-F, Supplemental Figure 2) (Filichkin
294 et al., 2011; Mockler et al., 2007). Also different from *AtELF3*, transcript levels of *BdELF3*
295 accumulate at dawn rather than peak in the evening (Supplemental Figure 2) when grown under
296 diel conditions, suggesting different regulations on *ELF3* expression between monocot and dicot
297 plants. Neither diel nor circadian expression data for *S. viridis* was available. Therefore, we
298 generated RNA-seq time-course data to examine *SvELF3* expression as well as the circadian
299 expression of other clock orthologs after both photocycle and thermocycle entrainment. In
300 addition, we developed the Diel Explorer tool
301 (<http://shiny.bioinformatics.danforthcenter.org/diel-explorer/>) to query and visualize *S. viridis*
302 circadian-regulated gene expression (Supplemental Figure 3). 48,594 *S. viridis* transcripts are
303 represented in the two datasets entrained under either photocycles (LDHH-F) or thermocycles
304 (LLHC-F). With Diel Explorer users can manually enter a list of transcript identifiers, gene
305 ontology (GO) terms, or gene orthologs, plot gene expression, and download data. Alternatively,

306 users can upload files of transcript identifiers or gene orthologs, and/or filter the datasets by
307 entrainment, phase, or significance cut-offs. Data and graphs can be downloaded directly using
308 Diel Explorer. The tool serves as a community resource that can be expanded to include other
309 circadian or diurnal data in the future. The underlying code is available on Github
310 (<https://github.com/maliagehan/diel-explorer>).

311
312 Under photoperiod entrainment (LDHH-F), 5,585 of the 48,594 *S. viridis* transcripts are
313 circadian regulated (Bonferroni-adjusted P-Value < 0.001). This proportion of photoperiod-
314 entrained circadian genes (~11.5%) is similar to maize (10.8%), rice (12.6%), and poplar
315 (11.2%) data sets, but much smaller than the approximately 30% reported for *A. thaliana*
316 (Covington et al., 2008; Filichkin et al., 2011; Khan et al., 2010). Under thermocycle
317 entrainment (LLHC-F), 582 of the 48,594 *S. viridis* transcripts are circadian regulated.
318 Therefore, only ~1.2% of *S. viridis* transcripts are circadian cycling under thermocycle
319 entrainment. The ~10-fold reduction in circadian cycling genes between photocycle and
320 thermocycle entrainment (Supplemental Figure 4) is interesting considering that there was less
321 than 1% difference in the number of genes with a circadian period between photocycle and
322 thermocycle entrainment in C3 monocot rice (*Oryza japonica*) (Filichkin et al., 2011). The
323 reduction in cycling genes between the two entrainment conditions in *S. viridis* compared to *O.*
324 *japonica* is an indication that circadian regulation could vary greatly among monocots. Also, the
325 difference in number of cycling genes between monocots and dicots may represent a significant
326 reduction of the role of the circadian clock between these lineages.

327
328 In addition to the overall reduction in circadian genes, the phase with the most number of cycling
329 genes was ZT18 after light entrainment (LDHH-F; Supplemental Figure 4), but ZT12 with
330 temperature entrainment (LLHC-F; Supplemental Figure 4), which is consistent with previous
331 studies that have found significant differences in temperature and light entrainment of the
332 circadian clock (Boikoglou et al., 2011; Michael et al., 2008; Michael et al., 2003). There are 269
333 genes that are considered circadian-regulated and are cycling under both LDHH-F and LLHC-F
334 conditions (Bonferroni Adjusted P-Value < 0.001). The list of 269 genes that overlap between
335 photocycle and thermocycle entrainment includes best matches for Arabidopsis core clock
336 components *TIMING OF CAB EXPRESSION 1* (*TOC1*, *AT5G61380.1*; *Sevir.1G241000.1*),
337 *LATE ELONGATED HYPOCOTYL* (*LHY*, *AT1G01060*; *Sevir.6G053100.1*), and *CCA1*-like gene
338 *REVEILLE1* (*RVE1*, *AT5G17300.1*; *Sevir.1G280700.1*). However, putative *S. viridis* orthologs of
339 *TOC1*, *LHY*, and *RVE1* all have different circadian phases under LDHH entrainment compared
340 to LLHC entrainment (Figure 1). In fact, the majority (233/269) of overlapping circadian genes
341 in *S. viridis* have a distinct circadian phase under thermocycle compared to photocycle entrainment
342 (Supplemental Figure 4). We also found that putative orthologs of *PSEUDO-RESPONSE*
343 *REGULATOR 7* (*PRR7*, *AT5G02810*; *Sevir.2G456400.1*; related to *OsPRR73* (Murakami et
344 al., 2003)) and *LUX ARRHYTHMO* (*LUX*, *AT3G46640*; *Sevir.5G474200.1*) cycle significantly

345 under LDHH-F but not LLHC-F conditions (Figure 1). Neither *SvELF3a* nor *SvELF3b* cycle
346 under circadian conditions after photo- or thermo-entrainment (Figure 1), similar to ELF3
347 orthologs in *B. distachyon* (Supplemental Figure 2) (Mockler et al., 2007) and *O. sativa*
348 (Filichkin et al., 2011). This is different from *AtELF3*, which continues to cycle under constant
349 condition after either photo- or thermos-entrainment (Supplemental Figure 5) (Mockler et al.,
350 2007). The difference in expression of these putative orthologs between *A. thaliana* and
351 monocots *S. viridis*, *B. distachyon*, and *O. sativa*, suggest that the architecture of the circadian
352 clock may have significant differences in response to environmental cues in these two species.

353

354 *BdELF3* and *SvELF3* Rescue Growth and Flowering Defects in *Arabidopsis elf3* Mutant.

355

356 Although the circadian expression pattern of *B. distachyon* *ELF3* and *S. viridis* *ELF3* is different
357 from that of *A. thaliana* *ELF3*, it is still possible that the ELF3 orthologs have conserved
358 biological functions. To test this, we sought to determine if *BdELF3* or *SvELF3a* could
359 complement the major phenotypic defects of the *elf3* mutant in *A. thaliana*, namely hypocotyl
360 elongation, time to flowering, or circadian rhythmicity. To this end, we constitutively expressed
361 *BdELF3*, *SvELF3a* (hereafter referred as *SvELF3*) and *AtELF3* cDNAs by the *35S Cauliflower*
362 *mosaic virus* promoter in the *A. thaliana elf3-2* mutant expressing a *LUCIFERASE* reporter
363 driven by the promoter of *CIRCADIAN CLOCK ASSOCIATED 1 (CCA1) (elf3-2 [CCA1:LUC])*
364 (Pruneda-Paz et al., 2009). All three ELF3 coding sequences were fused to a C-terminal His₆-
365 3xFlag affinity tag (HFC), which enables detection by western blotting and identification of
366 protein-protein interaction by affinity purification and mass spectrometry (AP-MS) (Huang et al.,
367 2016a). After transforming these constructs, we identified and selected two biologically
368 independent transgenic lines with a single insertion of each At/Bd/SvELF3-HFC construct.
369 Western blot analysis using FLAG antibodies detected the expression of all ELF3-HFC fusion
370 proteins (Supplemental Figure 6).

371

372 Next, we asked if expressing At/Bd/SvELF3-HFC fusion proteins could rescue the mutation
373 defects caused by *elf3-2*. When plants are grown under light/dark cycles (12 hour light: 12 hour
374 dark), *elf3-2* mutant plants elongate their hypocotyls much more than wild type plants (4.75 ± 0.48
375 mm vs. 1.95 ± 0.27 mm, respectively. \pm = standard deviation) (Figure 2). The long hypocotyl
376 defect in *elf3-2* was effectively suppressed by expressing either *AtELF3*, or *ELF3* orthologs
377 (*BdELF3* or *SvELF3a*) (Figure 2). These data show that the monocot *ELF3* orthologs function
378 similarly to *A. thaliana* *ELF3* in the regulation of hypocotyl elongation in seedlings.

379

380 In addition to regulating phenotypes in seedlings, ELF3 also functions in adult plants to suppress
381 the floral transition. Loss-of-function in *Arabidopsis* *ELF3* results in an early flowering
382 phenotype regardless of day-length (Hicks et al., 2001; Liu et al., 2001; Zagotta et al., 1992). To
383 determine how monocot ELF3 orthologs compared to *A. thaliana* *ELF3* in flowering time

384 regulation, we compared flowering responses under long day conditions among wild type, *elf3-2*,
385 and *elf3-2* transgenic lines expressing *AtELF3*, *BdELF3*, or *SvELF3* (At/Bd/SvELF3-HFC).
386 Constitutive over-expression of *AtELF3* led to a delay in flowering in long days (Figure 3) as
387 previously observed (Liu et al., 2001). Similarly, constitutive expression of *BdELF3* or *SvELF3*
388 caused plants to flower significantly later than the *elf3* mutants. These data show that all *ELF3*
389 orthologs can function to repress the rapid transition to flowering of the *elf3* mutation when
390 constitutively expressed in adult plants.

391

392 *BdELF3* and *SvELF3* Restore the Circadian Rhythmicity in *Arabidopsis elf3* Mutant.

393

394 *ELF3* is a key component of the *A. thaliana* circadian clock and is critical for maintaining the
395 periodicity and amplitude of rhythms as shown using the *CCA1* promoter driven luciferase
396 reporter (*CCA:LUC*) (Covington et al., 2001; Hicks et al., 1996; Nusinow et al., 2011). To
397 determine if *BdELF3* or *SvELF3a* could rescue the arrhythmic phenotype of the *elf3* mutation,
398 we analyzed the rhythms of the *CCA1::LUC* reporter under constant light conditions after diel
399 entrainment (12 hours light: 12 hours dark at constant 22 °C). Relative amplitude error (RAE)
400 analysis found that 100% of wild type and all three *elf3-2* transgenic lines expressing *AtELF3*,
401 *BdELF3*, and *SvELF3* were rhythmic, while only 50% of the *elf3-2* lines had rhythms (RAE <
402 0.5) (Supplemental Figure 7). Comparison of average period length found that the *AtELF3* and
403 *SvELF3* expressing lines rescued the period and amplitude defects in the *elf3* mutant (Figure 4A,
404 4C and 4D). While the *BdELF3* lines rescued the amplitude defect (Figure 4B), their period was
405 significantly divergent from wild type (compare 23.21 ± 0.59 hours for wild type to *BdELF3* #2=
406 26.03 ± 1.33 hours, *BdELF3* #3= 26.86 ± 0.81 hours, *elf3-2*= 26.54 ± 5.02 hours, \pm = standard
407 deviation, Figure 4D). In summary, these data show that expression of any of the *ELF3* orthologs
408 is sufficient to recover the amplitude and restore circadian rhythms of the *CCA1::LUC* reporter.

409

410 *BdELF3* and *SvELF3* are Integrated into a Similar Protein-Protein Interaction Network in *A.*
411 *thaliana*

412

413 Despite relatively low sequence conservation at the protein level, the *ELF3* orthologs can
414 complement a wide array of *elf3* phenotypes (Figures 2 to 4). As *ELF3* functions within the
415 evening complex (EC) in *Arabidopsis*, which also contains the transcription factor *LUX* and the
416 DUF-1313 domain containing protein *ELF4* (Herrero et al., 2012; Nusinow et al., 2011), we
417 reasoned that the monocot *ELF3* orthologs may also be able to bind to these proteins when
418 expressed in *A. thaliana*. To determine if a composite EC could be formed, we tested if *BdELF3*
419 or *SvELF3a* could directly interact with *AtLUX* or *AtELF4* in a yeast two-hybrid assay. Similar
420 to *AtELF3* (Nusinow et al., 2011), both *BdELF3* and *SvELF3a* directly interact with both
421 *AtELF4* and the C-terminal portion of *AtLUX* (Figure 5). We cannot conclude that whether

422 monocot ELF3 orthologs are also able to interact with the N-terminal AtLUX, since this
423 fragment auto-activated the reporter gene in the yeast two-hybrid assay (Figure 5).

424
425 ELF3 functions not only as the scaffold of the EC, but also as a hub protein in a protein-protein
426 interaction network containing multiple key regulators in both the circadian clock and light
427 signaling pathways (Huang et al., 2016a; Huang and Nusinow, 2016b). We hypothesize that
428 BdELF3 and SvELF3 could rescue many of the defects of the *elf3* mutant because both monocot
429 versions were integrated into the same protein-protein interaction network. To test this
430 hypothesis, we used affinity purification and mass spectrometry (AP-MS) to identify the proteins
431 that co-precipitate with monocot ELF3s when expressed in *A. thaliana*. AP-MS on two
432 biological replicates for each sample with the above-mentioned independent insertion lines were
433 included for each ELF3 ortholog. For comparison, the same AP-MS experiment was done with
434 one of the 35S promoter-driven AtELF3-HFC transgenic lines (AtELF3-2). To detect specific
435 co-precipitating proteins, we manually removed commonly identified contaminant proteins from
436 plant affinity purifications and mass spectrometry experiments (Van Leene et al., 2015), and
437 proteins identified from a control transgenic line expressing GFP-His₆-3xFlag described
438 previously (Huang et al., 2016b) (Table 1, the full list of identified proteins can be found in
439 Supplemental Table 2).

440
441 We have previously reported proteins that co-precipitated with ELF3 driven from its native
442 promoter using a similar AP-MS methodology (Huang et al., 2016a). When using the 35S
443 promoter driven AtELF3 transgenic line, we were able to generate a curated list of 22 proteins
444 that specifically co-precipitate with AtELF3, including all previously identified proteins, such as
445 all five phytochromes, PHOTOPERIODIC CONTROL OF HYPOCOTYL1 (PCH1), and COP1
446 (Table 1). In addition, we also identified LIGHT-REGULATED WD 2 (LWD2) and SPA1-
447 RELATED 4 (SPA4) as now co-precipitating with AtELF3. These additional interactions may be
448 a result of a combination of altered seedling age, expression level of the ELF3 bait, or tissue-
449 specificity of expression due to these purifications are from tissues where the epitope-tagged
450 transgene is constitutively over-expressed. However, since LWD2 is a known component of the
451 circadian clock (Wu et al., 2008) and SPA4 is a known component of the COP1-SPA complex
452 (Zhu et al., 2008), these interactions are likely to be relevant.

453
454 In comparing the list of BdELF3 and SvELF3 co-precipitated proteins with that of AtELF3, we
455 found that neither SvELF3 nor BdELF3 co-precipitated SPA2 and SPA4, components of the
456 COP1-SPA complex. In addition, SvELF3 did not co-precipitate MUT9-LIKE KINASE1, a
457 kinase with roles in chromatin modification and circadian rhythms as AtELF3 did (Huang et al.,
458 2016a; Wang et al., 2015). However, BdELF3 and SvELF3 associated with most of the proteins
459 found in AtELF3 AP-MS (20 out of 22 for BdELF3, 19 out of 22 for SvELF3), in at least one of
460 the replicate purifications from each monocot ortholog AP-MS. Therefore our data suggest that

461 BdELF3 and SvELF3 are integrated into a similar protein-protein interaction network as
462 AtELF3, which likely underlies their ability of broadly complementing *elf3* mutants.

463

464 Discussion

465

466 Recent work in diverse plant species has found that the circadian clock plays critical roles in
467 regulating metabolism, growth, photoperiodism, and other agriculturally important traits (Bendix
468 et al., 2015; McClung, 2013; Shor and Green, 2016). While the relevance of the circadian clock
469 to plant fitness is unquestioned, it is unclear if the circadian clock components have conserved
470 function among different plant species. This is particularly true for the majority of clock proteins,
471 whose biological functions are currently poorly understood at the molecular level (Hsu and
472 Harmer, 2014). Also, the divergent modes of growth regulation and photoperiodism between
473 monocots and dicots suggest that the clock evolved to have altered roles in regulating these
474 physiological responses between lineages (Matos et al., 2014; Poire et al., 2010; Song et al.,
475 2014). Here we asked if orthologs of ELF3 from two monocots could complement any of the
476 loss-of-function phenotypes in the model dicot plant *A. thaliana*. In this study we found that
477 ELF3 from either *B. distachyon* or *S. viridis* could complement the hypocotyl elongation, early
478 flowering, and arrhythmic clock phenotype of the *elf3* mutant in *A. thaliana*, despite the
479 variations in protein sequences and evolutionary divergence between monocot and dicot plants.
480 These data suggest that monocot ELF3s can functionally substitute for *A. thaliana* ELF3, albeit
481 with varying efficacy. Since monocot and dicot ELF3 are largely different in the protein
482 sequences, functional conservation of ELF3 orthologs also leads to the next open question of
483 identifying the functional domains within ELF3.

484

485 Previously, comparison of ELF3 homologs has identified at least five conserved regions that may
486 be important for function (Supplemental Figure 1) (Liu et al., 2001; Saito et al., 2012; Weller et
487 al., 2012). Our multiple sequence alignments also show that at least two regions of AtELF3,
488 namely the N-terminus (AA 1~49) and one middle region (AA 317~389) share many conserved
489 residues with ELF3 orthologs in grasses (Supplemental Figure 1). These regions fall within
490 known fragments that are sufficient for binding to phyB (Liu et al., 2001), COP1 (Yu et al.,
491 2008), or ELF4 (Herrero et al., 2012). Consistent with the hypothesis that these conserved
492 regions are critical for proper ELF3 function, a single amino acid substitution (A362V) within
493 this middle region results in defects of ELF3 nuclear localization and changes in the circadian
494 clock period (Anwer et al., 2014). In addition, our protein-protein interaction study and AP-MS
495 analysis show that both monocot ELF3 can form composite ECs (Figure 5) and that all three
496 ELF3 homologs interact with an almost identical set of proteins *in vivo* (Table 1), further
497 suggesting that one or more of the conserved regions may mediate the binding between ELF3
498 and its known interacting proteins. Furthermore, the similar pool of ELF3 interacting proteins
499 identified by Bd/SvELF3 AP-MS suggests that the overall conformation of ELF3 ortholog

500 proteins is conserved and that similar complexes and interactions with ELF3 orthologs may form
501 in monocot species. However, whether these interactions form *in planta* and have the same effect
502 on physiology is unclear. For example, *S. viridis* data generated here and public data for *B.*
503 *distachyon* and *O. sativa*, showed that ELF3 does not cycle under circadian conditions, which
504 differs from Arabidopsis. Further, different from the fact that the clock plays a key role in
505 regulating elongation in *A. thaliana* (Nozue et al., 2007), the circadian clock has no influence on
506 growth in C3 model grass *B. distachyon*, despite robust oscillating expression of putative clock
507 components (Matos et al., 2014). Similarly, ELF3 from rice (*Oryza sativa*) and soybean
508 promotes flowering and senescence (Lu et al., 2017; Saito et al., 2012; Sakuraba et al., 2016;
509 Yang et al., 2013; Zhao et al., 2012), while in *A. thaliana*, ELF3 represses these responses (Liu et
510 al., 2001; Sakuraba et al., 2014; Zagotta et al., 1992), which suggests significant rewiring of
511 ELF3 regulated photoperiodic responses of flowering between short-day (rice/soybean) and
512 long-day (*A. thaliana*) plants. Alternatively, ELF3 may form distinct interactions and complexes
513 in monocot species that were not identified in our trans-species complementation analysis.
514 Clearly, further work is required to understand ELF3 function in monocots beyond the studies
515 presented here.

516
517 In addition to the molecular characterization of ELF3, our analysis of circadian-regulated genes
518 in *S. viridis* after photo- and thermo-entrainment found significant differences in the behavior of
519 the clock when compared to other monocots. Although the number of circadian regulated genes
520 is comparable to studies done in corn and rice after photo-entrainment (between 10-12%)
521 (Filichkin et al., 2011; Khan et al., 2010), we found that very few genes (~1%) continue to cycle
522 after release from temperature entrainment in *S. viridis* (Supplemental Figure 4) when compared
523 to rice (~11%) (Filichkin et al., 2011). This may reflect a fundamental difference in how the
524 clock interfaces with temperature between these monocot species. Furthermore, proportions of
525 circadian regulated genes upon photo-entrainment in all three monocot plants (Supplement
526 Figure 4) (Filichkin et al., 2011; Khan et al., 2010) are much smaller than the approximately 30%
527 reported for *A. thaliana* (Covington et al., 2008), suggesting the divergence of clock functions
528 through evolution or domestication. Further comparisons of circadian responses among
529 monocots or between monocots and dicots will help to determine the molecular underpinning of
530 these differences.

531
532 In summary, we find that BdELF3 and SvELF3 form similar protein complexes *in vivo* as
533 AtELF3, which likely allows for functional complementation of loss-of-function of *elf3* despite
534 relatively low sequence conservation. We also present an online query tool, Diel Explorer that
535 allows for exploration of circadian gene expression in *S. viridis*, which illustrate fundamental
536 differences in clock function among monocots and between monocots and dicots. Collectively,
537 this work is a first step toward functional understanding of the circadian clock in two model
538 monocots, *S. viridis* and *B. distachyon*.

539

540 **Author contributions:** HH affinity purified ELF3 from transgenic lines, interpreted MS data
541 and measured protein interactions in yeast. MAG harvested and processed tissue to generate
542 libraries for RNA-seq, analyzed RNA-seq data, and generated Diel resource. SEH measured
543 hypocotyls, time to flowering, circadian rhythmicity, and analyzed transgenic lines by western
544 blot. SA assisted with developing MS methodology and spectral analysis. CL analyzed RNA-seq
545 data. ELG cloned Sv clock genes and characterized initial transgenic lines. JG designed and
546 verified the BdELF3 reagents. MJN processed samples and acquired the MS spectra. RB
547 identified and analyzed transgenic lines. BSE oversaw MS spectral data. DAN generated
548 AtELF3 lines and participated in circadian measurements. HH, MAG, TCM, and DAN
549 conceived the study. HH, MAG, and DAN wrote the manuscript. All authors edited the
550 manuscript.

551

552 **Conflict of Interest Statement:** The authors have no conflicts of interest to declare.

553

554 **Acknowledgments:** We acknowledge support from the NSF (DBI-0922879) for acquisition of
555 the LTQ-Velos Pro Orbitrap LC-MS/MS. T.C.M acknowledges support from the U.S.
556 Department of Energy ([DE-SC0006627](#), [DE-SC0012639](#), and [DE-SC0008769](#)) and M.A.G
557 acknowledges support from NSF-Plant Genome (IOS-1202682). D.A.N. acknowledges support
558 from the NSF (IOS-1456796).

559 **Figure legends**

560

561 **Figure 1. Circadian expression profiles of putative *S. viridis* clock components from Diel**
562 **Explorer using time-course RNA-seq data.** *S. viridis* plants were entrained by either
563 photocycle (LDHH) or thermocycle (LLHC), followed by being sampled every 2 hours for 48
564 hours under constant temperature and light conditions (Free-Running; F) to generate time-course
565 RNA-seq data. Mean values of Transcripts per Kilobase Million (TPM) from two experimental
566 replicates for each timepoints per gene were plotted.

567

568 **Figure 2. ELF3 orthologs suppress hypocotyl elongation defects in *elf3-2*.** The hypocotyls of
569 20 seedlings of wild type, *elf3-2* mutant, AtELF3 *elf3-2*, BdELF3 *elf3-2*, and SvELF3 *elf3-2* (two
570 independent transgenic lines for each ELF3 ortholog) were measured at 4 days after germination
571 under 12-hour light :12-hour dark growth conditions at 22 °C. Upper panel shows representative
572 seedlings of each genotype, with scale bar equal to 5 mm. Mean and 95% confidence intervals
573 are plotted as crosshairs. This experiment was repeated three times with similar results. ANOVA
574 analysis with Bonferroni correction was used to generate adjusted P values, * < 0.05, ** < 0.01,
575 **** < 0.0001.

576

577 **Figure 3. ELF3 orthologs suppress time to flowering of *elf3-2*.** 12 wild type, *elf3-2* mutant,
578 AtELF3 *elf3-2*, BdELF3 *elf3-2*, and SvELF3 *elf3-2* seedlings from two independent
579 transformations were measured for days (A) and number of rosette leaves (B) at flowering (1 cm
580 inflorescence). Mean and 95% confidence intervals are plotted as crosshairs. This experiment
581 was repeated twice with similar results. ANOVA analysis with Bonferroni correction was used to
582 generate adjusted P values, ** < 0.01, *** < 0.001, **** < 0.0001, of measurements when
583 compared to the *elf3-2* mutant line.

584

585 **Figure 4. ELF3 orthologs can recover *CCA1::LUC* rhythms and amplitude in *elf3-2***
586 **mutants.** 8 seedlings of wild type, *elf3-2* mutant, AtELF3 *elf3-2* (A), BdELF3 *elf3-2* (B), and
587 SvELF3 *elf3-2* (C) from two independent transformations were imaged for bioluminescence
588 under constant light after entrainment in 12-hour light :12-hour dark growth conditions at 22 °C.
589 Each plot shows average bioluminescence of all seedlings along with 95% confidence interval
590 (error bars). This experiment was repeated twice with similar results. Note that wild type and
591 *elf3-2* mutant data was plotted on all graphs for comparison. (D) Periods of seedlings. Only
592 periods with a Relative Amplitude Error below 0.5 (see Supplemental Figure 7) were plotted.
593 Mean and 95% confidence intervals are plotted as crosshairs. ANOVA analysis with Bonferroni
594 correction was used to generate adjusted P values, ** < 0.01, *** < 0.001, **** < 0.0001, of
595 measurements when compared to the wild type.

596

597 **Figure 5. Both BdELF3 and SvELF3 can directly bind to AtELF4 and AtLUX.** Yeast two-
598 hybrid analysis of testing if either BdELF3 (A) or SvELF3 (B) can directly interact with either
599 AtELF4, the N-terminal half of AtLUX (AtLUX-N, a.a. 1-143) or the C-terminal half of AtLUX
600 (AtLUX-C, a.a. 144-324). -LW tests for the presence of both bait (DBD) and pray (AD) vectors,
601 while the -LWH + 3AT tests for interaction. Vector alone serves as interaction control. This
602 experiment was repeated twice with similar results.

603
604
605
606
607
608
609
610
611
612
613
614
615
616
617
618
619
620
621
622
623
624
625
626
627
628
629
630
631
632
633
634
635
636
637
638
639
640
641
642
643
644
645
646

Table 1. Proteins co-purified with ELF3 orthologs from AP-MS.

Supplemental Table 1. **List of all primers used.**

Supplemental Table 2. **A full list of At/Bd/SvELF3 associated proteins identified from AP-MS.**

Supplemental Figure 1. **Multiple sequence alignments of ELF3 orthologs (A) and percentage of identical amino acid sequences (B).** Protein sequences of AtELF3 (AT2G25930.1), BdELF3 (Bradi2g14290.1), SvELF3a (Sevir.5G206400.1) and SvELF3b (Sevir.3G123200.1) were used for multiple sequence alignments and for generating percentage of identical amino acids by Clustal Omega alignment with default parameters.

Supplemental Figure 2. **Diel and circadian expression of *BdELF3* from the DIURNAL database.** GCRMA (GeneChip Robust Multiarray Averaging) values from the DIURNAL database (Mockler et al., 2007) were plotted to show time-course expression profiles of *Bradi2g14290 (BdELF3)* under either diel (A) or circadian conditions (B). Diel expression of *AtELF3* from DIURNAL database was used for comparison in (A). Shade boxes indicate dark periods. In (B), Circadian expression data was obtained by entraining plants with either photo- (LDHH) or thermo- (LLHC) conditions followed by sampling under the Free-Running condition (F) with constant light and temperature.

Supplemental Figure 3. **Example of the Diel Explorer interface.** The search interface (left) and plotting interface of Diel Explorer are shown (right). Users can search by gene or ortholog id, or by gene ontology term. Alternately, users can filter data by period, phase (lag) or significance cut offs. Data can be plotted in a line graph or heatmap.

Supplemental Figure 4. **Summary of circadian regulated genes in *S. viridis*.** Distribution of circadian regulated genes in *S. viridis* was plotted by their phases, with the y axis showing the number of genes considered significantly (Bonferroni Adjusted P-Value < 0.001) cycling under photo- (LDHH) or thermo- (LLHC) entrainment in *S. viridis* followed by free-running condition (F).

Supplemental Figure 5. **Circadian expression of selected *A. thaliana* clock genes from the DIURNAL database.** GCRMA (GeneChip Robust Multiarray Averaging) values were plotted to show time-course expression profiles of selected *A. thaliana* clock genes under either photo- (LL23_LDHH) or thermo-entrainment (LL_LLHC) from the DIURNAL database (Mockler et al., 2007). Each gene cycles with a correlation of > 0.9 when compared to a best fit model (24-hour rhythm).

Supplemental Figure 6. **Anti-FLAG western of ELF3 transgenic lines used for complementation analysis.** Representative blot of protein extracts from day 12 seedlings taken at Zeitgeber time 12 grown under 12-hour light :12-hour dark growth conditions at 22 °C that

647 were probed with FLAG antibody to detect the 3xFLAG epitope. RPT5 is used as a loading
648 control.

649

650 Supplemental Figure 7. **Relative Amplitude Error vs period plots.** The periods and relative
651 amplitude error (RAE) of 8 AtELF3 *elf3-2* (A), BdELF3 *elf3-2* (B), and SvELF3 *elf3-2* (C)
652 seedlings were plotted along with wild type and *elf3-2* mutants (Note, only 4 of 8 *elf3* seedlings
653 has measurable rhythms). RAE=0.5 was used as a cutoff (dotted line), above which a seedling is
654 not considered rhythmic (Plautz et al., 1997). Note that wild type and *elf3* mutant data were
655 reproduced on all plots for comparison purposes.

656

657

658 **References**

659

- 660 Altschul, S.F., Gish, W., Miller, W., Myers, E.W., and Lipman, D.J. (1990). Basic local
661 alignment search tool. *J Mol Biol* 215, 403-410.
- 662 Anwer, M.U., Boikoglou, E., Herrero, E., Hallstein, M., Davis, A.M., Velikkakam James, G.,
663 Nagy, F., and Davis, S.J. (2014). Natural variation reveals that intracellular distribution of ELF3
664 protein is associated with function in the circadian clock. *Elife* 3.
- 665 Bell-Pedersen, D., Cassone, V.M., Earnest, D.J., Golden, S.S., Hardin, P.E., Thomas, T.L., and
666 Zoran, M.J. (2005). Circadian rhythms from multiple oscillators: lessons from diverse organisms.
667 *Nat Rev Genet* 6, 544-556.
- 668 Bendix, C., Marshall, C.M., and Harmon, F.G. (2015). Circadian Clock Genes Universally
669 Control Key Agricultural Traits. *Mol Plant* 8, 1135-1152.
- 670 Bennetzen, J.L., Schmutz, J., Wang, H., Percifield, R., Hawkins, J., Pontaroli, A.C., Estep, M.,
671 Feng, L., Vaughn, J.N., Grimwood, J., *et al.* (2012). Reference genome sequence of the model
672 plant *Setaria*. *Nat Biotechnol* 30, 555-561.
- 673 Boikoglou, E., Ma, Z., von Korff, M., Davis, A.M., Nagy, F., and Davis, S.J. (2011).
674 Environmental memory from a circadian oscillator: the *Arabidopsis thaliana* clock differentially
675 integrates perception of photic vs. thermal entrainment. *Genetics* 189, 655-664.
- 676 Bray, N.L., Pimentel, H., Melsted, P., and Pachter, L. (2016). Near-optimal probabilistic RNA-
677 seq quantification. *Nat Biotech* 34, 525-527.
- 678 Brutnell, T.P., Wang, L., Swartwood, K., Goldschmidt, A., Jackson, D., Zhu, X.G., Kellogg, E.,
679 and Van Eck, J. (2010). *Setaria viridis*: a model for C4 photosynthesis. *Plant Cell* 22, 2537-2544.
- 680 Bushnell, B. (2016). BBMap short read aligner. University of California, Berkeley, California
681 URL <http://sourceforge.net/projects/bbmap>.
- 682 Calixto, C.P., Waugh, R., and Brown, J.W. (2015). Evolutionary relationships among barley and
683 *Arabidopsis* core circadian clock and clock-associated genes. *J Mol Evol* 80, 108-119.
- 684 Covington, M.F., Maloof, J.N., Straume, M., Kay, S.A., and Harmer, S.L. (2008). Global
685 transcriptome analysis reveals circadian regulation of key pathways in plant growth and
686 development. *Genome Biol* 9, R130.
- 687 Covington, M.F., Panda, S., Liu, X.L., Strayer, C.A., Wagner, D.R., and Kay, S.A. (2001). ELF3
688 modulates resetting of the circadian clock in *Arabidopsis*. *Plant Cell* 13, 1305-1315.

689 Dixon, L.E., Knox, K., Kozma-Bognar, L., Southern, M.M., Pokhilko, A., and Millar, A.J.
690 (2011). Temporal repression of core circadian genes is mediated through EARLY FLOWERING
691 3 in Arabidopsis. *Curr Biol* 21, 120-125.

692 Dodd, A.N., Salathia, N., Hall, A., Kevei, E., Toth, R., Nagy, F., Hibberd, J.M., Millar, A.J., and
693 Webb, A.A. (2005). Plant circadian clocks increase photosynthesis, growth, survival, and
694 competitive advantage. *Science* 309, 630-633.

695 Doherty, C.J., and Kay, S.A. (2010). Circadian control of global gene expression patterns. *Annu*
696 *Rev Genet* 44, 419-444.

697 Doyle, M.R., Davis, S.J., Bastow, R.M., McWatters, H.G., Kozma-Bognar, L., Nagy, F., Millar,
698 A.J., and Amasino, R.M. (2002). The ELF4 gene controls circadian rhythms and flowering time
699 in Arabidopsis thaliana. *Nature* 419, 74-77.

700 Edelstein, A., Amodaj, N., Hoover, K., Vale, R., and Stuurman, N. (2010). Computer control of
701 microscopes using microManager. *Curr Protoc Mol Biol Chapter 14*, Unit14 20.

702 Edelstein, A.D., Tsuchida, M.A., Amodaj, N., Pinkard, H., Vale, R.D., and Stuurman, N. (2014).
703 Advanced methods of microscope control using muManager software. *J Biol Methods* 1.

704 Edgar, R.S., Green, E.W., Zhao, Y., van Ooijen, G., Olmedo, M., Qin, X., Xu, Y., Pan, M.,
705 Valekunja, U.K., Feeney, K.A., *et al.* (2012). Peroxiredoxins are conserved markers of circadian
706 rhythms. *Nature* 485, 459-464.

707 Faure, S., Turner, A.S., Gruszka, D., Christodoulou, V., Davis, S.J., von Korff, M., and Laurie,
708 D.A. (2012). Mutation at the circadian clock gene EARLY MATURITY 8 adapts domesticated
709 barley (*Hordeum vulgare*) to short growing seasons. *Proc Natl Acad Sci U S A* 109, 8328-8333.

710 Filichkin, S.A., Breton, G., Priest, H.D., Dharmawardhana, P., Jaiswal, P., Fox, S.E., Michael,
711 T.P., Chory, J., Kay, S.A., and Mockler, T.C. (2011). Global Profiling of Rice and Poplar
712 Transcriptomes Highlights Key Conserved Circadian-Controlled Pathways and
713 *cis*-Regulatory Modules. *PLoS ONE* 6, e16907.

714 Goodstein, D.M., Shu, S., Howson, R., Neupane, R., Hayes, R.D., Fazo, J., Mitros, T., Dirks, W.,
715 Hellsten, U., Putnam, N., *et al.* (2012). Phytozome: a comparative platform for green plant
716 genomics. *Nucleic Acids Res* 40, D1178-1186.

717 Gould, P.D., Diaz, P., Hogben, C., Kusakina, J., Salem, R., Hartwell, J., and Hall, A. (2009).
718 Delayed fluorescence as a universal tool for the measurement of circadian rhythms in higher
719 plants. *Plant J* 58, 893-901.

720 Graf, A., Schlereth, A., Stitt, M., and Smith, A.M. (2010). Circadian control of carbohydrate
721 availability for growth in Arabidopsis plants at night. *Proc Natl Acad Sci U S A* 107, 9458-9463.

722 Greenham, K., and McClung, C.R. (2015). Integrating circadian dynamics with physiological
723 processes in plants. *Nat Rev Genet* 16, 598-610.

724 Harmer, S.L. (2009). The circadian system in higher plants. *Annu Rev Plant Biol* 60, 357-377.

725 Harmer, S.L., Hogenesch, J.B., Straume, M., Chang, H.S., Han, B., Zhu, T., Wang, X., Kreps,
726 J.A., and Kay, S.A. (2000). Orchestrated transcription of key pathways in Arabidopsis by the
727 circadian clock. *Science* 290, 2110-2113.

728 Hazen, S.P., Schultz, T.F., Pruneda-Paz, J.L., Borevitz, J.O., Ecker, J.R., and Kay, S.A. (2005).
729 LUX ARRHYTHMO encodes a Myb domain protein essential for circadian rhythms. *Proc Natl*
730 *Acad Sci U S A* 102, 10387-10392.

- 731 Helfer, A., Nusinow, D.A., Chow, B.Y., Gehrke, A.R., Bulyk, M.L., and Kay, S.A. (2011). LUX
732 ARRHYTHMO encodes a nighttime repressor of circadian gene expression in the Arabidopsis
733 core clock. *Curr Biol* 21, 126-133.
- 734 Herrero, E., Kolmos, E., Bujdoso, N., Yuan, Y., Wang, M., Berns, M.C., Uhlworm, H.,
735 Coupland, G., Saini, R., Jaskolski, M., *et al.* (2012). EARLY FLOWERING4 recruitment of
736 EARLY FLOWERING3 in the nucleus sustains the Arabidopsis circadian clock. *Plant Cell* 24,
737 428-443.
- 738 Hicks, K.A., Albertson, T.M., and Wagner, D.R. (2001). EARLY FLOWERING3 encodes a
739 novel protein that regulates circadian clock function and flowering in Arabidopsis. *Plant Cell* 13,
740 1281-1292.
- 741 Hicks, K.A., Millar, A.J., Carre, I.A., Somers, D.E., Straume, M., Meeks-Wagner, D.R., and
742 Kay, S.A. (1996). Conditional circadian dysfunction of the Arabidopsis early-flowering 3
743 mutant. *Science* 274, 790-792.
- 744 Higgins, J.A., Bailey, P.C., and Laurie, D.A. (2010). Comparative genomics of flowering time
745 pathways using *Brachypodium distachyon* as a model for the temperate grasses. *PLoS One* 5,
746 e10065.
- 747 Hsu, P.Y., and Harmer, S.L. (2014). Wheels within wheels: the plant circadian system. *Trends in*
748 *plant science* 19, 240-249.
- 749 Huang, H., Alvarez, S., Bindbeutel, R., Shen, Z., Naldrett, M.J., Evans, B.S., Briggs, S.P., Hicks,
750 L.M., Kay, S.A., and Nusinow, D. (2016a). Identification of Evening Complex Associated
751 Proteins in Arabidopsis by Affinity Purification and Mass Spectrometry. *Mol Cell Proteomics*
752 15, 201-217.
- 753 Huang, H., Alvarez, S., Bindbeutel, R., Shen, Z., Naldrett, M.J., Evans, B.S., Briggs, S.P., Hicks,
754 L.M., Kay, S.A., and Nusinow, D.A. (2016b). Identification of Evening Complex Associated
755 Proteins in Arabidopsis by Affinity Purification and Mass Spectrometry. *Mol Cell Proteomics*
756 15, 201-217.
- 757 Huang, H., and Nusinow, D. (2016a). Tandem Purification of His6-3x FLAG Tagged Proteins
758 for Mass Spectrometry from Arabidopsis. *Bio-Protocol* 6.
- 759 Huang, H., and Nusinow, D.A. (2016b). Into the Evening: Complex Interactions in the
760 Arabidopsis Circadian Clock. *Trends Genet* 32, 674-686.
- 761 Huang, H., Yoo, C.Y., Bindbeutel, R., and Goldsworthy, J. (2016c). PCH1 integrates circadian
762 and light-signaling pathways to control photoperiod-responsive growth in Arabidopsis. *eLife*.
- 763 Hughes, M.E., Hogenesch, J.B., and Kornacker, K. (2010). JTK_CYCLE: an efficient
764 nonparametric algorithm for detecting rhythmic components in genome-scale data sets. *J Biol*
765 *Rhythms* 25, 372-380.
- 766 Keller, A., Nesvizhskii, A.I., Kolker, E., and Aebersold, R. (2002). Empirical Statistical Model
767 To Estimate the Accuracy of Peptide Identifications Made by MS/MS and Database Search.
768 *Analytical Chemistry* 74, 5383-5392.
- 769 Khan, S., Rowe, S.C., and Harmon, F.G. (2010). Coordination of the maize transcriptome by a
770 conserved circadian clock. *BMC Plant Biol* 10, 126.
- 771 Khanna, R., Kikis, E.A., and Quail, P.H. (2003). EARLY FLOWERING 4 functions in
772 phytochrome B-regulated seedling de-etiolation. *Plant Physiol* 133, 1530-1538.

773 Kim, W.Y., Hicks, K.A., and Somers, D.E. (2005). Independent roles for EARLY FLOWERING
774 3 and ZEITLUPE in the control of circadian timing, hypocotyl length, and flowering time. *Plant*
775 *Physiol* 139, 1557-1569.

776 Kolmos, E., Herrero, E., Bujdoso, N., Millar, A.J., Toth, R., Gyula, P., Nagy, F., and Davis, S.J.
777 (2011). A reduced-function allele reveals that EARLY FLOWERING3 repressive action on the
778 circadian clock is modulated by phytochrome signals in *Arabidopsis*. *Plant Cell* 23, 3230-3246.

779 Kumar, R., Ichihashi, Y., Kimura, S., Chitwood, D.H., Headland, L.R., Peng, J., Maloof, J.N.,
780 and Sinha, N.R. (2012). A High-Throughput Method for Illumina RNA-Seq Library Preparation.
781 *Front Plant Sci* 3, 202.

782 Liu, X.L., Covington, M.F., Fankhauser, C., Chory, J., and Wagner, D.R. (2001). ELF3 encodes
783 a circadian clock-regulated nuclear protein that functions in an *Arabidopsis* PHYB signal
784 transduction pathway. *Plant Cell* 13, 1293-1304.

785 Lou, P., Wu, J., Cheng, F., Cressman, L.G., Wang, X., and McClung, C.R. (2012). Preferential
786 retention of circadian clock genes during diploidization following whole genome triplication in
787 *Brassica rapa*. *Plant Cell* 24, 2415-2426.

788 Lu, S., Zhao, X., Hu, Y., Liu, S., Nan, H., Li, X., Fang, C., Cao, D., Shi, X., Kong, L., *et al.*
789 (2017). Natural variation at the soybean J locus improves adaptation to the tropics and enhances
790 yield. *Nat Genet.*

791 Matos, D.A., Cole, B.J., Whitney, I.P., MacKinnon, K.J., Kay, S.A., and Hazen, S.P. (2014).
792 Daily changes in temperature, not the circadian clock, regulate growth rate in *Brachypodium*
793 *distachyon*. *PLoS One* 9, e100072.

794 Matsubara, K., Ogiso-Tanaka, E., Hori, K., Ebana, K., Ando, T., and Yano, M. (2012). Natural
795 variation in Hd17, a homolog of *Arabidopsis* ELF3 that is involved in rice photoperiodic
796 flowering. *Plant Cell Physiol* 53, 709-716.

797 McClung, C.R. (2013). Beyond *Arabidopsis*: the circadian clock in non-model plant species.
798 *Semin Cell Dev Biol* 24, 430-436.

799 Michael, T.P., Mockler, T.C., Breton, G., McEntee, C., and Byer, A. (2008). Network discovery
800 pipeline elucidates conserved time-of-day-specific cis-regulatory modules. *PLoS genetics.*

801 Michael, T.P., Salome, P.A., and McClung, C.R. (2003). Two *Arabidopsis* circadian oscillators
802 can be distinguished by differential temperature sensitivity. *Proc Natl Acad Sci U S A* 100,
803 6878-6883.

804 Mizuno, T., Nomoto, Y., Oka, H., Kitayama, M., Takeuchi, A., Tsubouchi, M., and Yamashino,
805 T. (2014). Ambient temperature signal feeds into the circadian clock transcriptional circuitry
806 through the EC night-time repressor in *Arabidopsis thaliana*. *Plant Cell Physiol* 55, 958-976.

807 Mockler, T.C., Michael, T.P., Priest, H.D., Shen, R., Sullivan, C.M., Givan, S.A., McEntee, C.,
808 Kay, S.A., and Chory, J. (2007). The DIURNAL project: DIURNAL and circadian expression
809 profiling, model-based pattern matching, and promoter analysis. *Cold Spring Harb Symp Quant*
810 *Biol* 72, 353-363.

811 Murakami, M., Ashikari, M., Miura, K., Yamashino, T., and Mizuno, T. (2003). The
812 Evolutionarily Conserved OsPRR Quintet: Rice Pseudo-Response Regulators Implicated in
813 Circadian Rhythm. *Plant and Cell Physiology* 44, 1229-1236.

814 Nagel, D.H., and Kay, S.A. (2012). Complexity in the wiring and regulation of plant circadian
815 networks. *Curr Biol* 22, R648-657.

816 Nesvizhskii, A.I., Keller, A., Kolker, E., and Aebersold, R. (2003). A Statistical Model for
817 Identifying Proteins by Tandem Mass Spectrometry. *Analytical Chemistry* 75, 4646-4658.

818 Nozue, K., Covington, M.F., Duek, P.D., Lorrain, S., Fankhauser, C., Harmer, S.L., and Maloof,
819 J.N. (2007). Rhythmic growth explained by coincidence between internal and external cues.
820 *Nature* 448, 358-361.

821 Nusinow, D.A., Helfer, A., Hamilton, E.E., King, J.J., Imaizumi, T., Schultz, T.F., Farre, E.M.,
822 and Kay, S.A. (2011). The ELF4-ELF3-LUX complex links the circadian clock to diurnal
823 control of hypocotyl growth. *Nature* 475, 398-402.

824 Onai, K., and Ishiura, M. (2005). PHYTOCLOCK 1 encoding a novel GARP protein essential
825 for the Arabidopsis circadian clock. *Genes Cells* 10, 963-972.

826 Ouyang, Y., Andersson, C.R., Kondo, T., Golden, S.S., and Johnson, C.H. (1998). Resonating
827 circadian clocks enhance fitness in cyanobacteria. *Proc Natl Acad Sci U S A* 95, 8660-8664.

828 Plautz, J.D., Straume, M., Stanewsky, R., Jamison, C.F., Brandes, C., Dowse, H.B., Hall, J.C.,
829 and Kay, S.A. (1997). Quantitative Analysis of Drosophila period Gene Transcription in Living
830 Animals. *Journal of Biological Rhythms* 12, 204-217.

831 Poire, R., Wiese-Klinkenberg, A., Parent, B., Mielewczik, M., Schurr, U., Tardieu, F., and
832 Walter, A. (2010). Diel time-courses of leaf growth in monocot and dicot species: endogenous
833 rhythms and temperature effects. *J Exp Bot* 61, 1751-1759.

834 Pokhilko, A., Fernandez, A.P., Edwards, K.D., Southern, M.M., Halliday, K.J., and Millar, A.J.
835 (2012). The clock gene circuit in Arabidopsis includes a repressilator with additional feedback
836 loops. *Mol Syst Biol* 8, 574.

837 Pruneda-Paz, J.L., Breton, G., Para, A., and Kay, S.A. (2009). A functional genomics approach
838 reveals CHE as a component of the Arabidopsis circadian clock. *Science* 323, 1481-1485.

839 Saito, H., Ogiso-Tanaka, E., Okumoto, Y., Yoshitake, Y., Izumi, H., Yokoo, T., Matsubara, K.,
840 Hori, K., Yano, M., Inoue, H., *et al.* (2012). Ef7 encodes an ELF3-like protein and promotes rice
841 flowering by negatively regulating the floral repressor gene Ghd7 under both short- and long-day
842 conditions. *Plant Cell Physiol* 53, 717-728.

843 Sakuraba, Y., Han, S.H., Yang, H.J., Piao, W., and Paek, N.C. (2016). Mutation of Rice Early
844 Flowering3.1 (OsELF3.1) delays leaf senescence in rice. *Plant Mol Biol*.

845 Sakuraba, Y., Jeong, J., Kang, M.Y., Kim, J., Paek, N.C., and Choi, G. (2014). Phytochrome-
846 interacting transcription factors PIF4 and PIF5 induce leaf senescence in Arabidopsis. *Nat*
847 *Commun* 5, 4636.

848 Schneider, C.A., Rasband, W.S., and Eliceiri, K.W. (2012). NIH Image to ImageJ: 25 years of
849 image analysis. *Nat Meth* 9, 671-675.

850 Shor, E., and Green, R.M. (2016). The Impact of Domestication on the Circadian Clock. *Trends*
851 *Plant Sci* 21, 281-283.

852 Sievers, F., Wilm, A., Dineen, D., Gibson, T.J., Karplus, K., Li, W., Lopez, R., McWilliam, H.,
853 Remmert, M., Soding, J., *et al.* (2011). Fast, scalable generation of high-quality protein multiple
854 sequence alignments using Clustal Omega. *Mol Syst Biol* 7, 539.

855 Song, Y.H., Ito, S., and Imaizumi, T. (2010). Similarities in the circadian clock and
856 photoperiodism in plants. *Curr Opin Plant Biol* 13, 594-603.

857 Song, Y.H., Shim, J.S., Kinmonth-Schultz, H.A., and Imaizumi, T. (2014). Photoperiodic
858 Flowering: Time Measurement Mechanisms in Leaves. *Annu Rev Plant Biol*.

859 Van Leene, J., Eeckhout, D., Cannoot, B., De Winne, N., Persiau, G., Van De Slijke, E.,
860 Vercruyse, L., Dedecker, M., Verkest, A., Vandepoele, K., *et al.* (2015). An improved toolbox
861 to unravel the plant cellular machinery by tandem affinity purification of Arabidopsis protein
862 complexes. *Nat Protocols* 10, 169-187.

863 Vizcaino, J.A., Deutsch, E.W., Wang, R., Csordas, A., Reisinger, F., Rios, D., Dianes, J.A., Sun,
864 Z., Farrah, T., Bandeira, N., *et al.* (2014). ProteomeXchange provides globally coordinated
865 proteomics data submission and dissemination. *Nat Biotechnol* 32, 223-226.

866 Wang, L., Si, Y., Dedow, L.K., Shao, Y., Liu, P., and Brutnell, T.P. (2011a). A low-cost library
867 construction protocol and data analysis pipeline for Illumina-based strand-specific multiplex
868 RNA-seq. *PLoS One* 6, e26426.

869 Wang, W., Barnaby, J.Y., Tada, Y., Li, H., Tor, M., Caldelari, D., Lee, D.U., Fu, X.D., and
870 Dong, X. (2011b). Timing of plant immune responses by a central circadian regulator. *Nature*
871 470, 110-114.

872 Wang, Z., Casas-Mollano, J.A., Xu, J., Riethoven, J.J., Zhang, C., and Cerutti, H. (2015).
873 Osmotic stress induces phosphorylation of histone H3 at threonine 3 in pericentromeric regions
874 of *Arabidopsis thaliana*. *Proc Natl Acad Sci U S A* 112, 8487-8492.

875 Weller, J.L., Liew, L.C., Hecht, V.F.G., Rajandran, V., Laurie, R.E., Ridge, S., Wenden, B.,
876 Vander Schoor, J.K., Jaminon, O., Blassiau, C., *et al.* (2012). A conserved molecular basis for
877 photoperiod adaptation in two temperate legumes. *Proc Natl Acad Sci U S A* 109, 21158-21163.

878 Wijnen, H., and Young, M.W. (2006). Interplay of circadian clocks and metabolic rhythms.
879 *Annu Rev Genet* 40, 409-448.

880 Woelfle, M.A., Ouyang, Y., Phanvijhitsiri, K., and Johnson, C.H. (2004). The adaptive value of
881 circadian clocks: an experimental assessment in cyanobacteria. *Curr Biol* 14, 1481-1486.

882 Wu, J.F., Wang, Y., and Wu, S.H. (2008). Two new clock proteins, LWD1 and LWD2, regulate
883 *Arabidopsis* photoperiodic flowering. *Plant Physiol* 148, 948-959.

884 Yang, Y., Peng, Q., Chen, G.-X., Li, X.-H., and Wu, C.-Y. (2013). OsELF3 is involved in
885 circadian clock regulation for promoting flowering under long-day conditions in rice. *Mol Plant*
886 6, 202-215.

887 Yu, J.W., Rubio, V., Lee, N.Y., Bai, S., Lee, S.Y., Kim, S.S., Liu, L., Zhang, Y., Irigoyen, M.L.,
888 Sullivan, J.A., *et al.* (2008). COP1 and ELF3 control circadian function and photoperiodic
889 flowering by regulating GI stability. *Mol Cell* 32, 617-630.

890 Zagotta, M., Shannon, S., Jacobs, C., and Meeks-Wagner, D. (1992). Early-Flowering Mutants
891 of *Arabidopsis thaliana*. *Functional Plant Biology* 19, 411-418.

892 Zakhrabekova, S., Gough, S.P., Braumann, I., Muller, A.H., Lundqvist, J., Ahmann, K., Dockter,
893 C., Matyszcak, I., Kurowska, M., Druka, A., *et al.* (2012). Induced mutations in circadian clock
894 regulator Mat-a facilitated short-season adaptation and range extension in cultivated barley. *Proc*
895 *Natl Acad Sci U S A* 109, 4326-4331.

896 Zhang, X., Henriques, R., Lin, S.-S., Niu, Q.-W., and Chua, N.-H. (2006). Agrobacterium-
897 mediated transformation of *Arabidopsis thaliana* using the floral dip method. *Nat Protocols* 1,
898 641-646.

899 Zhao, J., Huang, X., Ouyang, X., Chen, W., Du, A., Zhu, L., Wang, S., Deng, X.W., and Li, S.
900 (2012). OsELF3-1, an ortholog of *Arabidopsis* early flowering 3, regulates rice circadian rhythm
901 and photoperiodic flowering. *PLoS One* 7, e43705.

902 Zhu, D., Maier, A., Lee, J.H., Laubinger, S., Saijo, Y., Wang, H., Qu, L.J., Hoecker, U., and
903 Deng, X.W. (2008). Biochemical characterization of Arabidopsis complexes containing
904 CONSTITUTIVELY PHOTOMORPHOGENIC1 and SUPPRESSOR OF PHYA proteins in
905 light control of plant development. *Plant Cell* 20, 2307-2323.
906

Figure 1

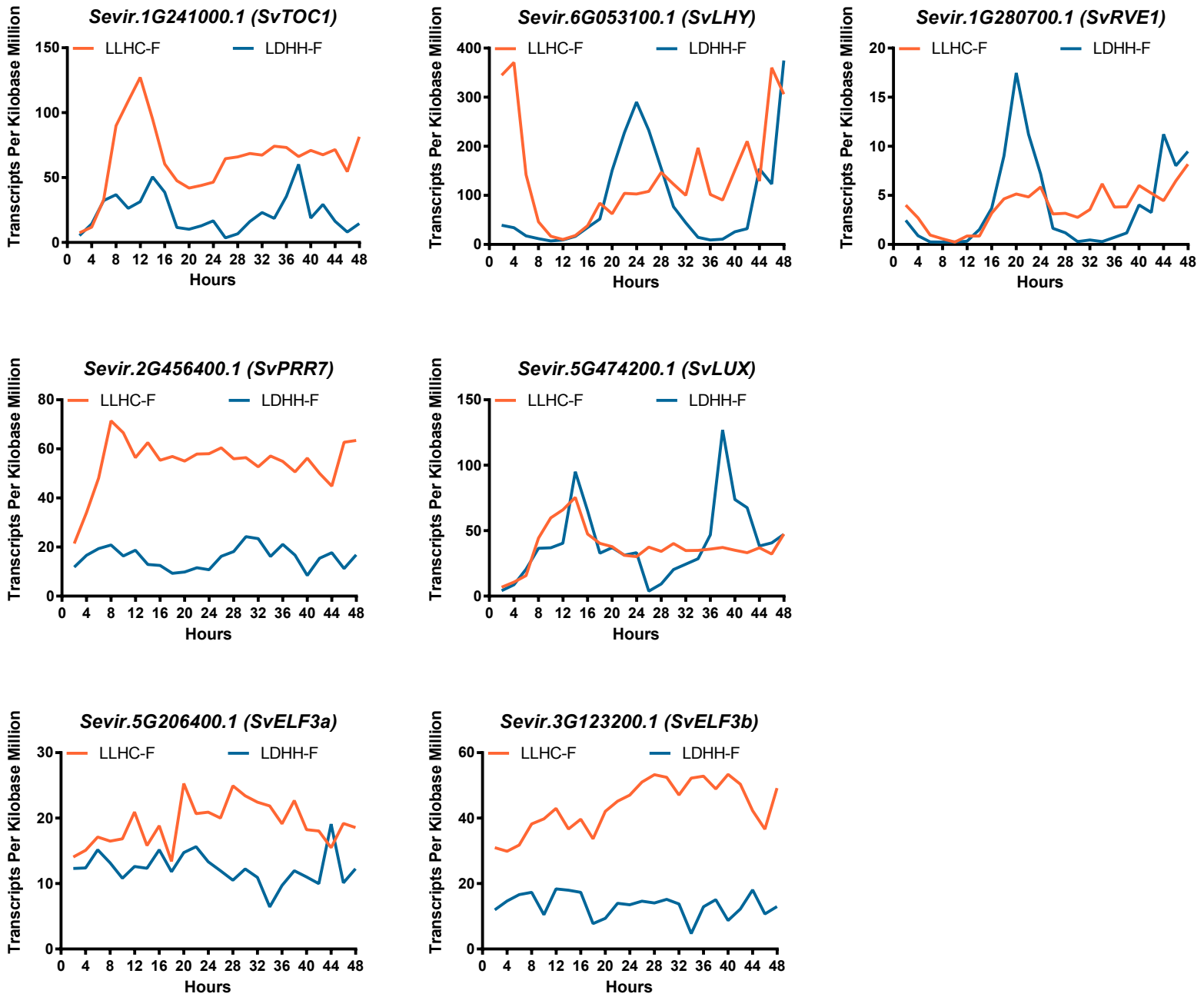


Figure 2

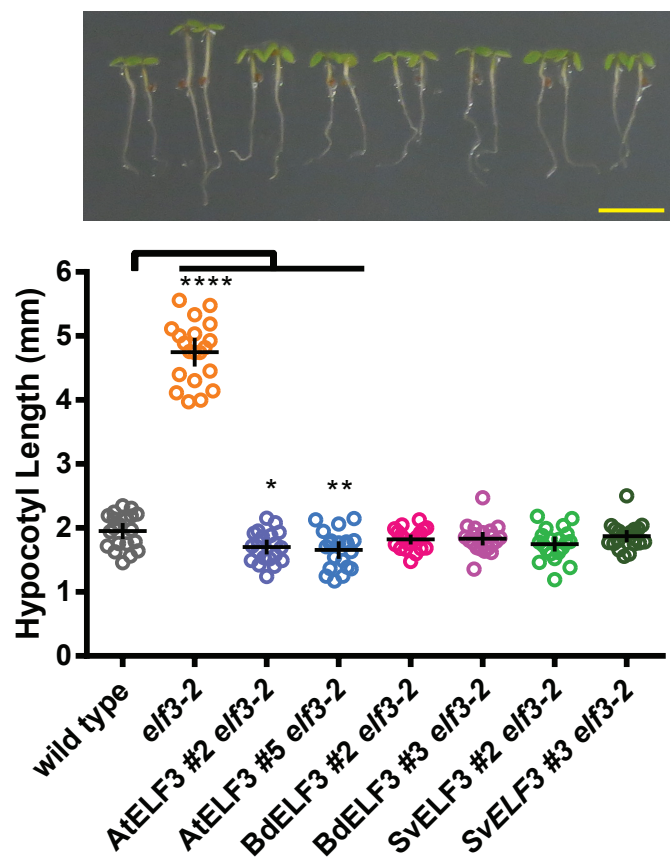


Figure 3

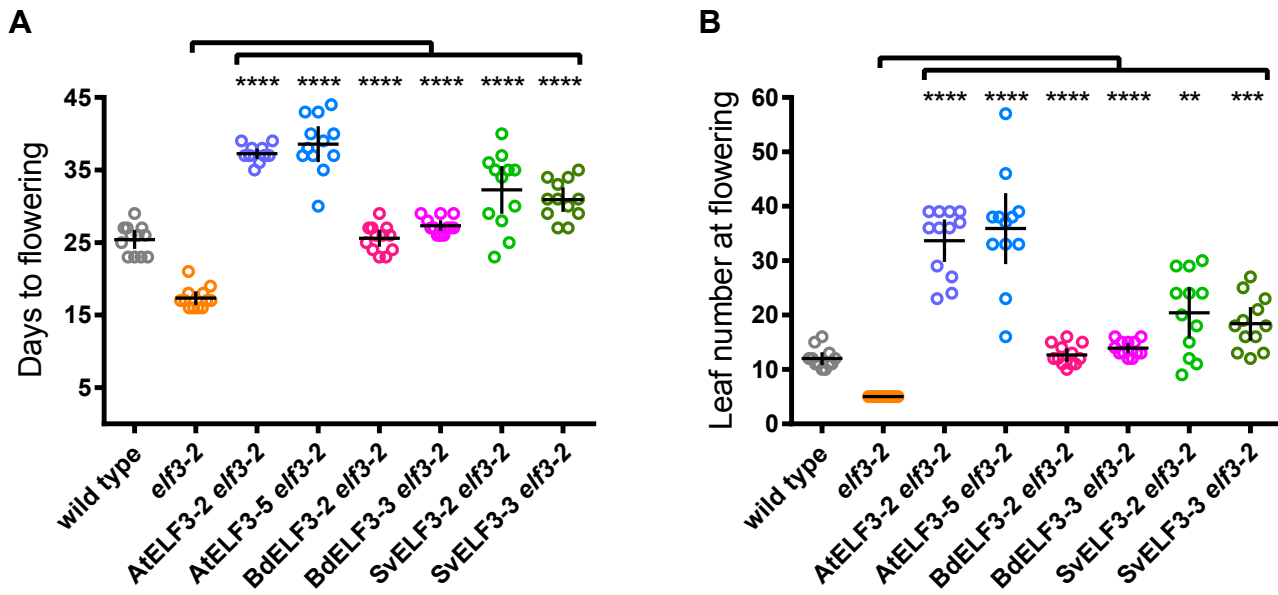


Figure 4

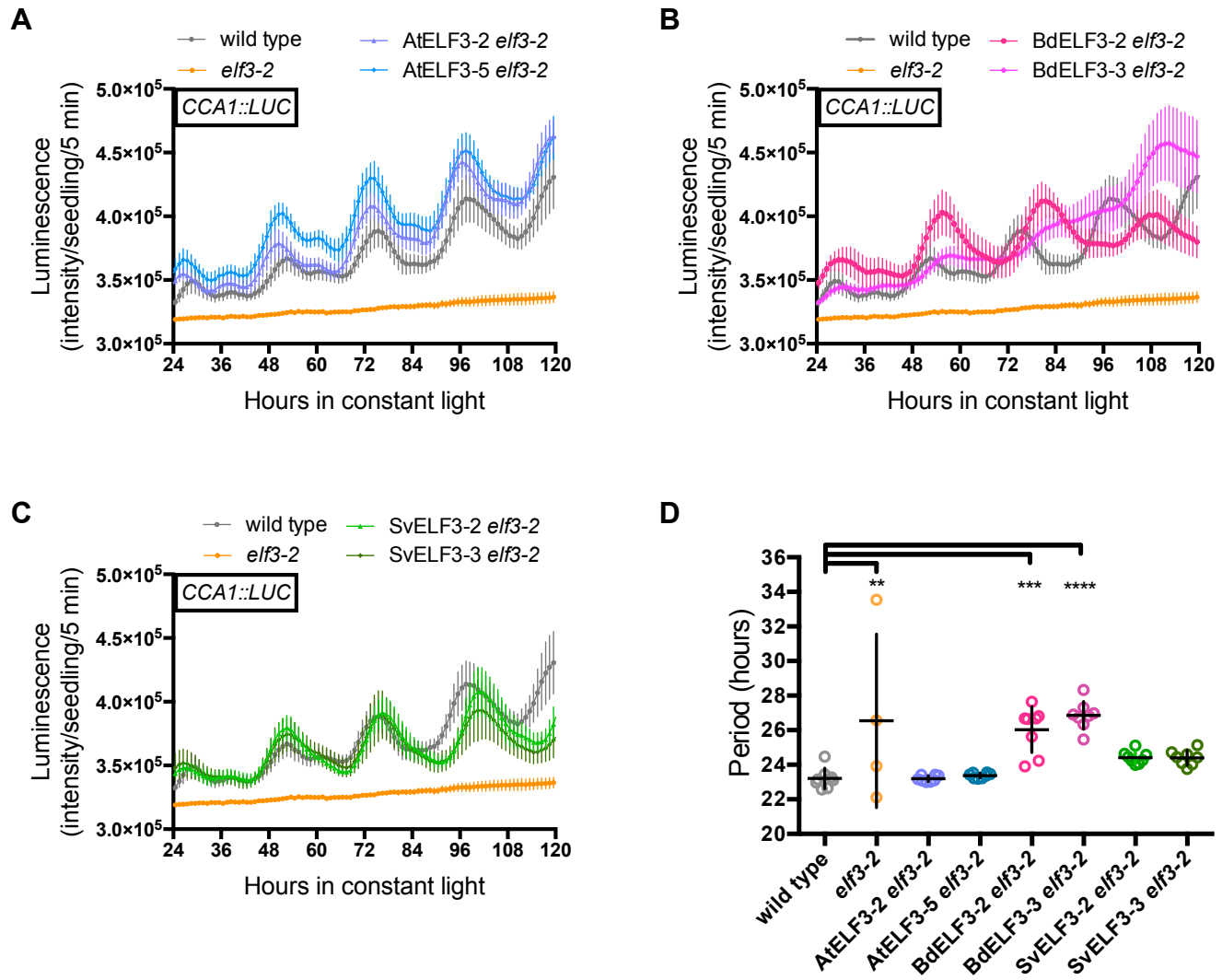


Figure 5

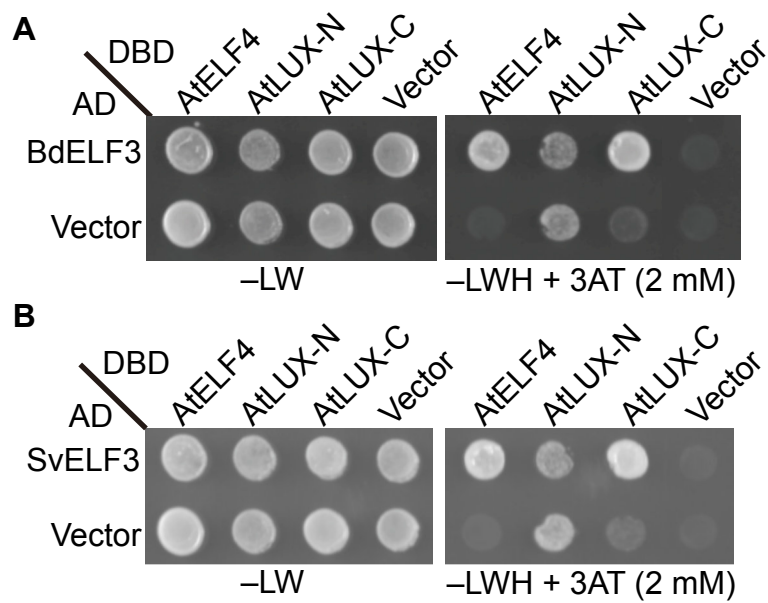


Table 1. Proteins co-purified with ELF3 orthologs from AP-MS

AGI number	Protein Name	Molecular Weight	Exclusive Unique Peptide Count/Percent Coverage ^a									
			AtELF3		SvELF3 #2		SvELF3 #3		BdELF3 #2		BdELF3 #3	
			rep1	rep2	rep1	rep2	rep1	rep2	rep1	rep2	rep1	rep2
n/a	AtELF3-HFC	84 kDa	20/36%	19/31%	—	—	—	—	—	—	—	—
n/a	SvELF3-HFC	87 kDa	—	—	19/40%	29/48%	22/42%	33/54%	—	—	—	—
n/a	BdELF3-HFC	86 kDa	—	—	—	—	—	—	25/42%	26/43%	21/35%	19/33%
AT2G18790	phyB	129 kDa	23/37%	24/37%	31/54%	28/42%	32/50%	30/45%	22/34%	22/33%	24/40%	24/37%
AT5G35840	phyC	124 kDa	22/29%	23/29%	27/37%	32/39%	27/37%	33/42%	20/24%	18/22%	19/23%	22/27%
AT5G43630	TZP	91 kDa	14/21%	12/17%	13/23%	20/33%	13/22%	24/36%	12/18%	13/19%	14/20%	14/22%
AT4G18130	phyE	123 kDa	11/16%	19/27%	12/18%	18/23%	11/19%	17/24%	6/7%	10/14%	14/19%	13/18%
AT2G16365.2	PCH1 ^b	51 kDa	9/25%	9/25%	9/30%	14/43%	11/36%	16/49%	9/26%	9/28%	11/32%	11/32%
AT2G46340	SPA1	115 kDa	8/14%	7/9%	2/2%	4/8%	2/3%	4/9%	—	—	6/8%	5/6%
AT3G42170 ^c	DAYSLLEEPER	79 kDa	8/19%	5/11%	—	7/16%	—	12/27%	3/7%	4/8%	2/4%	—
AT2G32950	COP1	76 kDa	8/16%	9/17%	6/17%	4/8%	3/6%	5/12%	1/2%	2/4%	6/11%	4/8%
AT3G22380	TIC	165 kDa	5/5%	5/5%	4/4%	12/12%	3/3%	15/15%	4/4%	3/3%	1/1%	1/1%
AT4G11110	SPA2	115 kDa	5/11%	6/12%	—	—	—	—	—	—	—	—
AT2G40080	ELF4	12 kDa	4/50%	4/50%	3/42%	5/68%	4/60%	4/60%	4/50%	4/50%	5/68%	5/68%
AT1G09340 ^c	CRB	43 kDa	4/16%	3/12%	1/4%	1/4%	1/4%	4/18%	1/4%	1/4%	—	—
AT3G13670	MLK4	79 kDa	3/10%	3/13%	—	—	—	1/2%	6/21%	3/10%	3/11%	5/13%
AT5G61380	TOC1	69 kDa	2/4%	2/4%	2/5%	—	3/7%	—	—	—	1/2%	1/2%
AT1G53090	SPA4	89 kDa	2/6%	5/14%	—	—	—	—	—	—	—	—
AT5G18190	MLK1	77 kDa	2/12%	2/11%	—	—	—	—	2/14%	2/14%	2/11%	2/11%
AT3G26640	LWD2	39 kDa	2/21%	1/21%	—	1/16%	—	2/22%	3/27%	1/16%	—	—
AT1G12910	LWD1	39 kDa	2/21%	3/30%	2/21%	4/31%	1/17%	2/21%	2/22%	2/19%	0/11%	0/11%
AT4G16250	phyD	129 kDa	1/10%	1/11%	2/12%	1/12%	3/15%	2/12%	2/11%	1/10%	2/14%	2/12%
AT1G09570	phyA	125 kDa	1/1%	1/1%	7/11%	5/5%	7/11%	2/2%	—	2/2%	6/7%	3/4%
AT2G25760	MLK3	76 kDa	1/5%	1/6%	—	1/4%	—	1/4%	3/13%	2/9%	2/9%	2/9%
AT3G03940	MLK2	78 kDa	1/8%	1/8%	—	1/7%	—	0/2%	3/20%	2/13%	3/13%	1/9%
AT3G46640	LUX	35 kDa	1/3%	1/3%	0/10%	3/19%	0/10%	3/23%	1/3%	1/3%	1/3%	2/11%
AT1G17455	ELF4-L4	13 kDa	—	—	—	—	—	—	1/23%	1/23%	—	—
AT1G72630	ELF4-L2	13 kDa	—	1/11%	—	1/13%	—	—	1/22%	1/22%	1/22%	1/11%

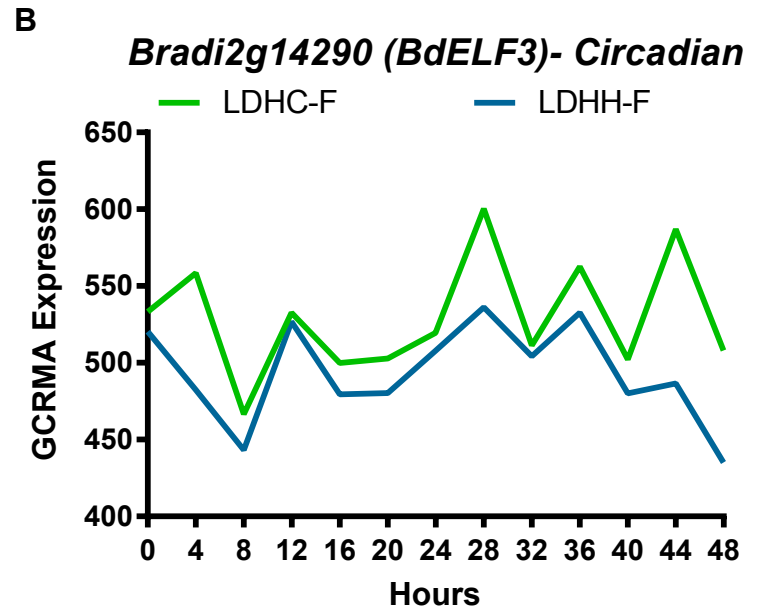
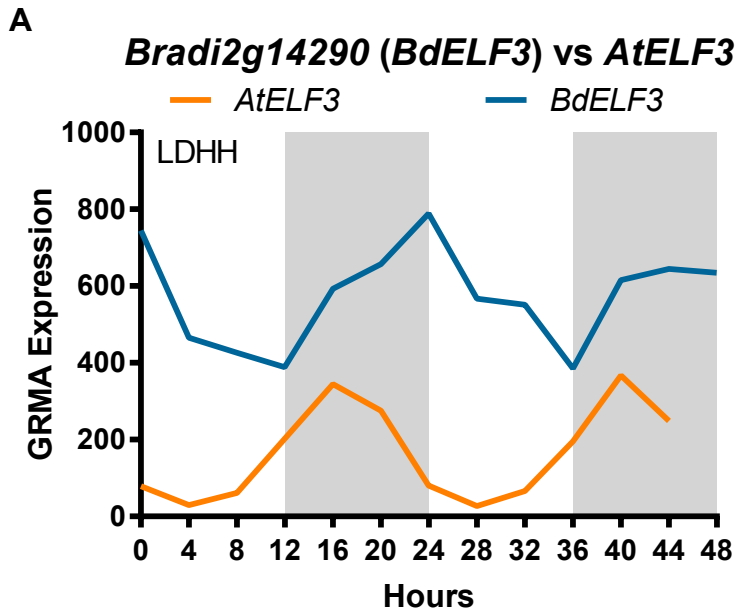
Proteins co-purified with ELF3 orthologs (AtELF3, SvELF3 and BdELF3, with C-terminal His₆-3xFLAG tag) were identified from affinity purification coupled with mass spectrometry (AP-MS) analyses using 12L:12D grown, 10-day-old transgenic plants (in *elf3-2 null* mutant backgrounds) harvested at ZT12.

^a All listed proteins match 99% protein threshold, minimum number peptides of 2 and peptide threshold as 95%. Proteins not matching the criteria were marked with "—".

^b percent coverage for PCH1 is calculated using protein encoded by *At2g16365.2*

^c These proteins have been noted as frequently identified proteins in AP-MS experiments (see Van Leene, 2015).

Supplemental Figure 2



Diel Explorer

Welcome Sample Info Search and Browse Data Plot Data Adding Your Own Data Contact Us

Search Data with GENEID or GO

Search using small sets of GENEIDS
GENEIDs, Orthologs, or GO separated by a comma are allowed
example: *Sevir:2G310Z00.1, Sevir:1G000100.1*

Search using small sets of GO TERMS
example: *GO:00:0008270*

Search using small sets of ORTHOLOG GENEIDS
example: *AT3G17930.1,LOC_001g59080.1*

refresh page to clear search

Search Data with File

Genes, Orthologs, or GO Selected with Search

Browse and Filter Data

Normalize Data: Yes NO
Species: All
Entrainment: Idh1f
Benjamin-Hochberg Q-Value: 1e-06
Adjusted P-Value: 1e-06
Period: All
Lag (Phase): 2
Download Selected Data

Show 25 entries

GENEID	BH Q	ADLP	PERIOD	LAG	AMPLITUDE	dataset	species	locusName
<i>Sevir:1G324600.1</i>	5.52e-09	4.37e-11	26	2	195.869285	Idh1f	setaria.viridis	<i>Sevir:1G324600</i>
<i>Sevir:2G080100.1</i>	5.05e-07	9.95e-09	26	2	17.908540	Idh1f	setaria.viridis	<i>Sevir:2G080100</i>
<i>Sevir:2G310Z00.1</i>	1.01e-12	5.19e-16	26	2	5909.517645	Idh1f	setaria.viridis	<i>Sevir:2G310Z00</i>
<i>Sevir:3G255600.1</i>	6.17e-08	8.12e-10	26	2	173.735429	Idh1f	setaria.viridis	<i>Sevir:3G255600</i>
<i>Sevir:5G333300.1</i>	3.07e-08	3.54e-10	26	2	3.692540	Idh1f	setaria.viridis	<i>Sevir:5G333300</i>
<i>Sevir:6G185200.1</i>	4.70e-09	3.65e-11	24	2	1.399562	Idh1f	setaria.viridis	<i>Sevir:6G185200</i>
<i>Sevir:9G089300.1</i>	2.31e-08	2.52e-10	26	2	3.249368	Idh1f	setaria.viridis	<i>Sevir:9G089300</i>
<i>Sevir:9G175700.1</i>	4.18e-10	1.73e-12	26	2	1316.979309	Idh1f	setaria.viridis	<i>Sevir:9G175700</i>
<i>Sevir:9G369500.1</i>	1.01e-07	2.50e-09	28	2	2.346460	Idh1f	setaria.viridis	<i>Sevir:9G369500</i>

Showing 1 to 9 of 9 entries

Previous 1 Next

Diel Explorer

Welcome Sample Info Search and Browse Data Plot Data Adding Your Own Data Contact Us

Plot Data

Warning: Attempting to plot too much data on line graph will be slow/unresponsive and messy.

Plot Selected Data as Line Graph Plot Selected Data as Heatmap

Color Line Graph By: Dataset GENEID

Scale Heatmap: Row Column

Average Replicates: Yes No

Download Line Graph Download Heatmap

Expression of Relative Expression

factor(unquoted)

- Sevir:1G324600* -Idh1f
- Sevir:2G080100* -Idh1f
- Sevir:2G310Z00* -Idh1f
- Sevir:3G255600* -Idh1f
- Sevir:5G333300* -Idh1f
- Sevir:6G185200* -Idh1f
- Sevir:9G089300* -Idh1f
- Sevir:9G175700* -Idh1f
- Sevir:9G369500* -Idh1f

shape

- REF1
- REF2

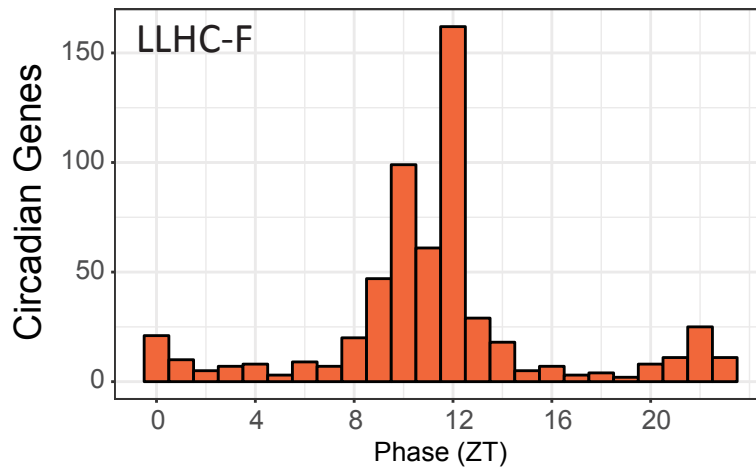
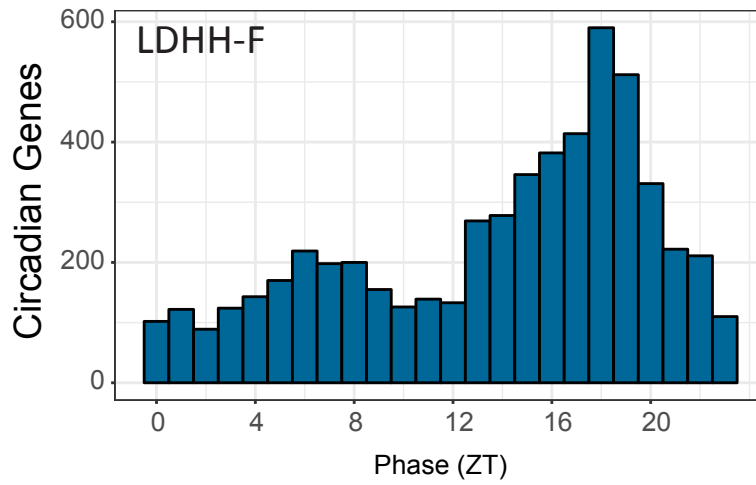
Heatmap

TIME(ZT)

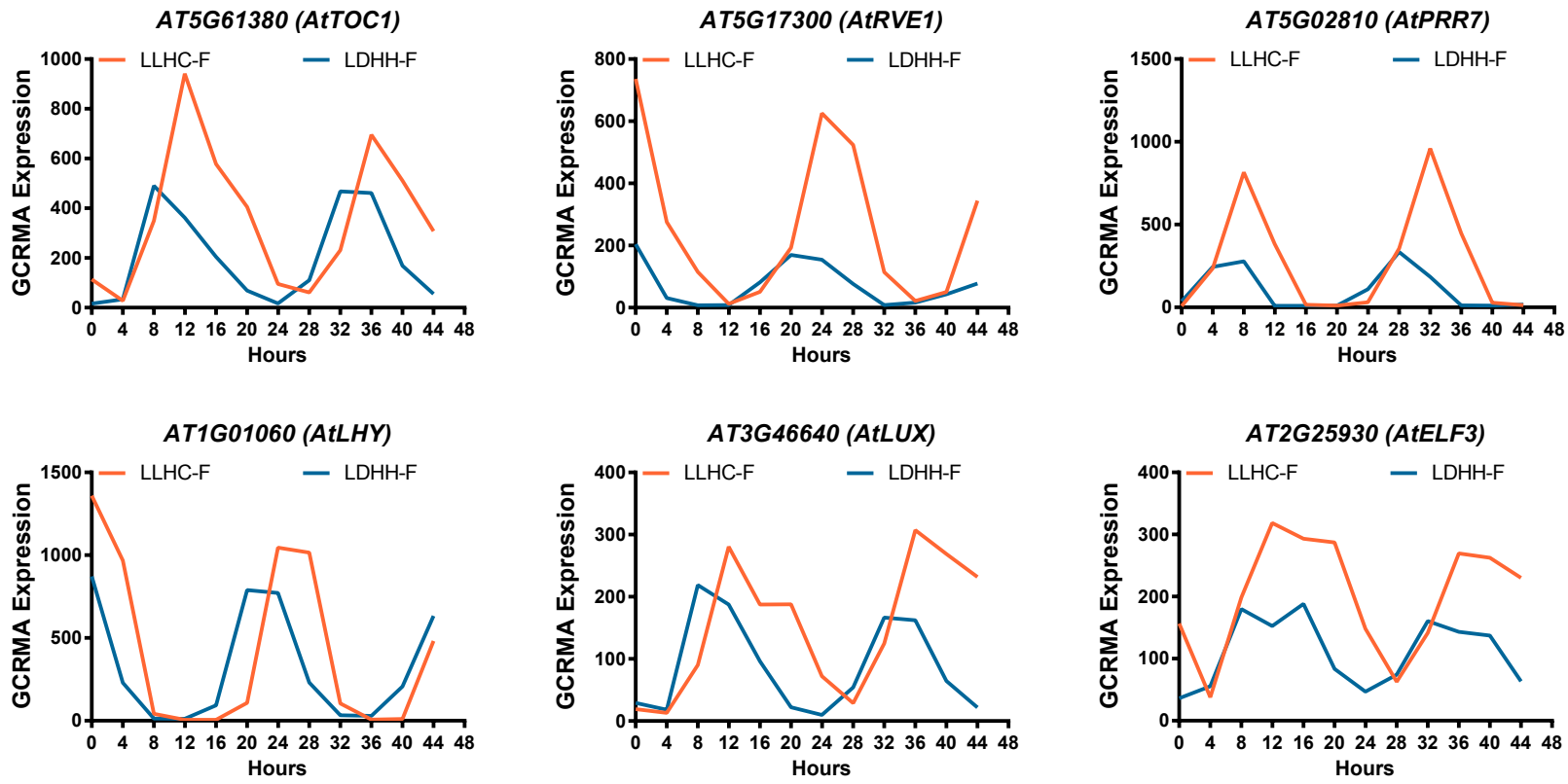
1 0 -1

Supplemental Figure 4

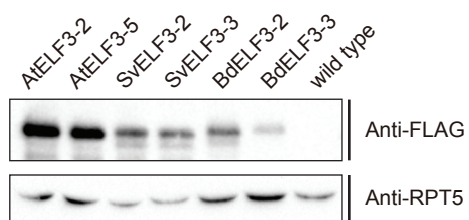
Phase of Circadian Genes in *S. viridis*



Supplemental Figure 5



Supplemental Figure 6



Supplemental Figure 7

